
OXIDATIVE FIXATION *of* DINITROGEN
***by* PHOTOCATALYSIS**

by

Fatiema Karriem



UNIVERSITY *of the*
WESTERN CAPE

A thesis in partial fulfillment for the degree of
Master of Science in the Department of Chemistry,
University of the Western Cape.

SUPERVISOR: Dr. D. L. KEY

2000

ACKNOWLEDGEMENTS

My heartfelt thanks to THE ALMIGHTY ALLAH who has bestowed upon me his richest blessings, so that I am able to partially understand his creation. I would also like to thank ALLAH for enriching my life with the people I will mention below.

I hereby wish to thank my supervisor, Dr. D. L. Key, for affording me the opportunity to engage in the photocatalysis research described here. I greatly appreciate the professional assistance he has given me.

To my family, especially my mother whose encouragement and support have really motivated me through all my years of study.

To my colleagues and friends in the chemistry department, as well as in the mathematics department, for just being there. To all my other friends for their moral support.

To my bursars, viz., FRD and Richards Bay Minerals (RBM) for their financial support, especially to Mr. John Selby from RBM who has been so understanding and kind throughout the duration of my research.

ABBREVIATIONS

1. Titanium dioxide	TiO ₂
2. Hydrogen peroxide	H ₂ O ₂
3. Sodium hydroxide	NaOH
4. Sulphuric acid	H ₂ SO ₄
5. Ammonia	NH ₃
6. Scanning Electron-Microscopy	SEM
7. Fourier Transform Infra-red Spectroscopy	FTIR
8. Ultraviolet - Visible Spectroscopy	Vis/UV
9. Richards Bay Minerals	RBM
10. Below detection limit range	LO



ABSTRACT

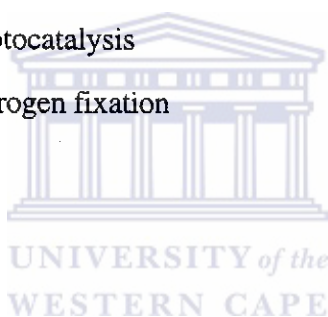
The heterogeneous photocatalytic oxidation of dinitrogen to nitrate, NO_3^- and/or nitrite, NO_2^- using peroxy species of titanium (IV) in aqueous suspensions has been investigated. The photocatalysts used were titanium peroxide and Degussa P25 TiO_2 pretreated with H_2O_2 . These photocatalysts were investigated by SEM and FTIR spectroscopy.

The photocatalysts were suspended in an aqueous solution and irradiated with visible or ultraviolet light while passing air through the suspension. The resulting NO_3^- concentrations determined indicate that oxidative fixation of dinitrogen does occur. The results indicate that the Degussa P25 TiO_2 pretreated with H_2O_2 is a better photocatalyst than titanium peroxide. The former photocatalyst was further investigated with variation of irradiation times, pH-values, masses of photocatalyst in suspension, concentration of H_2O_2 and wavelength of light in order to establish conditions for maximization of the NO_3^- concentration. The concentrations of NO_3^- obtained under the optimum conditions used are a significant improvement on previously reported results.

RBM rutile samples also appear to act as photocatalysts for the fixation of dinitrogen.

TABLE OF CONTENTS

	<u>Page No.</u>
1. INTRODUCTION	
1.1 Titanium	1
1.2 Titanium dioxide, TiO ₂ as a semiconductor	2
1.3 TiO ₂ as a photocatalyst	11
1.4 Nitrogen fixation	14
1.5 Nitrogen fixation in nature	16
1.5.1 Nitrogen in agriculture	19
1.6 Nitrogen fixation as an industrial process	21
1.7 Photocatalytic reactions using TiO ₂ as a photocatalyst	24
1.8 Nitrogen fixation using photocatalysis	25
1.9 Photocatalytic oxidative nitrogen fixation	28
2. OBJECTIVES	
2.1 Aim	31
2.2 Background Theory	31
3. EXPERIMENTAL	
3.1 Material used	35
3.2 Catalyst Preparation	35
3.2.1 Preparation of titanium peroxide compounds	35
3.2.2 Preparation of H ₂ O ₂ treated Degussa P25, TiO ₂	37
3.2.3 Preparation of H ₂ O ₂ treated RBM rutile flour	37
3.2.4 Preparation of H ₂ O ₂ treated RBM concentrated rutile	37



3.3	Catalyst Characterisation	38
3.3.1	General uses of molecular spectroscopy	38
3.3.2	Fourier Transform Infra-red Spectroscopy (FTIR)	38
3.3.3	Scanning Electron Microscopy (SEM)	42
3.3.4	Ultraviolet - Visible Spectroscopy (Vis/UV)	45
3.4	Irradiation Experiments	47
3.4.1	Schematic diagram of experimental apparatus	47
3.4.1.1	Reaction vessel	47
3.4.1.2	Xenon lamp	47
3.4.1.3	UV lamp	47
3.4.2	Irradiation procedure	48
3.5	Nitrate, NO_3^- and Nitrite, NO_2^- Analysis	48
3.5.1	Qualitative analysis	48
3.5.1.1	Test for NO_3^-	48
3.5.1.2	Test for NO_2^-	49
3.5.2	Quantitative analysis	49
3.5.2.1	Nitrate test strip analyser	51
3.5.2.2	Nitrite test strip analyser	53



4. RESULTS and DISCUSSION of CATALYST CHARACTERISATION

4.1	FTIR Studies on peroxo titanium compounds	55
4.1.1	Introduction	55
4.1.2	Results	56
4.2	Bandgap energies using the Vis/UV spectroscopy	57
4.3	Morphology analysis of the catalysts	62

5. RESULTS and DISCUSSION of IRRADIATION EXPERIMENTS	
5.1 Effect of using different solid compounds as catalysts	66
5.1.1 Comparison of the different forms of titanium peroxide	66
5.1.2 Degussa P25, TiO ₂	67
5.1.3 Comparing the effect of the uses of different photocatalysts	68
5.2 Blank Experiments -	69
5.2.1 Requirement of a solid photocatalyst	70
5.2.2 Requirement of air	70
5.2.3 Requirement of irradiation	71
5.2.4 Effect of the Xenon and UV lamp irradiation	72
5.2.5 Summary	73
5.3 Investigation of further variables on oxidative nitrogen fixation using Degussa P25 as photocatalyst	74
5.3.1 Effect of different pH-values	74
5.3.2 Effect of the concentration of H ₂ O ₂	76
5.3.3 Effect of mass of catalyst	78
5.3.4 Summary	79
5.4 Use of RBM rutile samples as photocatalysts	79
6. CONCLUSION	81
7. REFERENCES	82

LIST OF FIGURES

	<u>Page No</u>
1. Band structure of a metal	4
2. Band structure of an insulator	5
3. Illustration of a semiconductor, indicating the filled valence band and empty conduction band with a small gap.	5
4. Mechanism of charge generation (a) Thermal generation, (b) Photo-excitation, (c) Doping, n-type and (d) Doping, p-type.	6
5. The band theory diagram for an n-type semiconductor	9
6. The band theory diagram for a p-type semiconductor	9
7. Structure of the TiO ₂ (a) rutile and (b) anatase	12
8. Indication of “top 14” chemicals produced by the industry	14
9. Nitrogen cycle	17
10. Part of the plant used in the synthesis of ammonia	23
11. The energy level diagram of TiO ₂	32
12. The Perkin - Elmer Diffuse Reflectance Accessory	42
13. Schematic diagram of a SEM	43
14. Experimental set-up	47
15. FTIR spectra of the titanium peroxide compound prepared by Method I	57
16. The Vis/UV spectra of the titanium peroxide compound prepared by Method.I	58
17. The Vis/UV spectrum of the Degussa P25	59
18. The Vis/UV spectrum of TiO ₂ (rutile)	60
19. Electron micrograph of Degussa P25	63
20. Electron micrograph of RBM rutile flour	64
21. Electron micrograph of RBM concentrated rutile	65
22. Comparison of the Degussa P25 and titanium peroxide used as photocatalysts.	68

23. The effect of different pH-values using Degussa P25 as the photocatalyst.
Irradiation was carried out using the Xenon lamp passing air through
a 90ml sample at 1500ml/min. 75
24. The effect of the concentration of H₂O₂ using Degussa P25 as the photocatalyst
at pH 4. Irradiation was carried out using a Xenon lamp. 77
25. The effect of the mass of catalyst (Degussa P25) at pH 4 using the Xenon
lamp for irradiation. Air was passed through a 90ml sample at 1500ml/min. 78
26. The use of RBM rutile samples as photocatalysts at pH 4. Irradiation was carried
out using the Xenon lamp passing air through a 90ml sample at 1500ml/min. 80



LIST OF TABLES

	<u>Page No.</u>
1. Classification of semiconducting metal oxides	11
2. Special advantages of FTIR spectroscopy	40
3. Analysis of nitrate concentration (ppm) by nitrate test strip and two other analytical methods	50
4. The RQflex reflectometer measuring range of the nitrite test strips.	51
5. The RQflex reflectometer measuring range of the nitrate test strips.	53
6. The bandgap energies and wavelengths of some possible catalysts obtained from the Vis/UV spectra.	63
7. Concentration of NO_3^- and NO_2^- obtained using titanium peroxide compounds (conditions described in section 3.2.1) as the photocatalyst. Irradiation was carried out using the Xenon lamp passing air through a 90ml sample at 1500ml/min.	66
8. Concentration of NO_3^- and NO_2^- using Degussa P25 (conditions described in section 3.2.2) as the photocatalyst. Irradiation was carried out using the Xenon lamp passing air through a 90ml sample at 1500ml/min.	67
9. Concentration of NO_3^- and NO_2^- obtained where no catalyst was used at pH 14. Irradiation was carried out using the Xenon lamp.	70
10. Concentration of NO_3^- and NO_2^- obtained using the Degussa P25 (conditions described in section 3.2.2) as a photocatalyst irradiated with the Xenon lamp.	71
11. NO_3^- and NO_2^- concentration obtained using Degussa P25 (conditions described in section 3.2.2). Irradiation was carried out using the Xenon lamp passing air through a 90ml sample at 1500ml/min..	72
12. Concentration of NO_3^- and NO_2^- obtained with variation of the irradiation source (i.e. Xenon and UV lamp).	73

Chapter 1

INTRODUCTION



UNIVERSITY *of the*
WESTERN CAPE

1.1 TITANIUM

Titanium is the ninth most abundant element in the earth's crust.¹ Titanium is a hundred times as abundant in nature as such common elements as copper, lead and zinc. The annual world production of titanium pigments is over 100,000 tons and has grown very rapidly in recent years.² Titanium is a greyish metal and resembles in tin in its chemical properties.³

There are two important forms of titanium minerals in nature, namely ilmenite and rutile. The former is much more abundant, which has an approximate formula of the oxide of titanium and iron, FeTiO_3 , while the latter is nearly pure TiO_2 and thus a more desirable ore.¹ Primary ilmenite deposits are magmatic segregations or veins derived therefrom; primary rutile occurs in a number of ways, segregations in igneous rocks such as syenite, anorthosite and gabbro, and in pegmatitic rocks of various kinds.³ Most of the exploited deposits of both minerals, however, are of detrital character, such as beach-sands.

The most important compound of titanium is the dioxide. This occurs in nature but it must generally be purified before use. Titanium dioxide is also prepared from ilmenite via the action of hydrogen chloride and chlorine to form TiCl_4 followed by hydrolysis.²

Pure titanium dioxide is a white powder, insoluble in water and very resistant to corroding influences.² It is used on a very large scale as a white pigment.² TiO_2 has three different crystal structures, namely rutile, anatase and brookite.³

There is hardly a white-colored or tinted object in our environment and that includes the paper on which these words are printed that does not contain TiO_2 pigments. These compounds, whose chemical name is titanium (IV) oxide or titanium dioxide, is manufactured in enormous quantities.⁵

Titanium dioxide is used for exterior paints because of its chemical inertness, superior covering power, opacity to damaging ultraviolet (UV) light and non-toxic qualities.⁴ Both the rutile and anatase form are used, but especially the former.

The dioxide has also been used as whitening or opacifying agent in numerous situations. Examples would be the use a filter paper, colouring agent for rubber and leather products, a pigment in ink, and a component of ceramics. It has found important use as an opacifying agent in porcelain enamels, giving a finish coat of great brilliance, hardness, and acid resistance.⁴

1.2 TITANIUM DIOXIDE, TiO_2 , AS A SEMICONDUCTOR

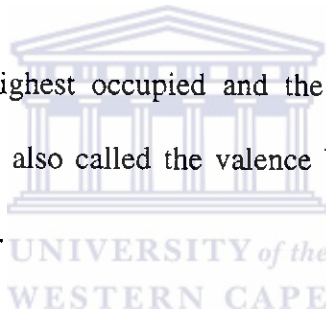
Although transition metal oxides have been known for a long time, in the last decade there has been an increasing interest in them due to their important role in heterogeneous catalysis. It has long been recognised that there are many reactions, which can be promoted by light-activated solids, which are not consumed in the overall reaction; such solids are often referred to as photocatalysis, or photosensitisers, and are invariably semiconductors.

More recently in material science, where high temperature superconductors have attracted much attention amongst research groups from all over the world.⁶ The electrical characteristics of solids can be described at room temperature and at atmospheric pressure under one of the following headings: (i) metals, (ii) insulators or (iii) semiconductors, intrinsic and extrinsic (n-type and p-type).

The differences between metals, semiconductors and insulators depend on:

- (a) the band structure of each,
- (b) whether the valence band are full or only partly full,
- (c) the magnitude of any energy gap between full and empty bands.

Of particular interest are the highest occupied and the lowest empty bands. The highest occupied energy band is also called the valence band and the lowest empty energy band the conduction band.



Metals^{7, 8} are characterised by a band structure in which the highest occupied band, the valence band is only partially filled. The occupied levels are shown schematically by the shading, some levels just below the Fermi level are vacant whereas some above E_F are occupied. A metal will characteristically possess a high electrical conductivity, which decreases as the temperature increases.

In metals, empty levels are available immediately above the filled ones, and at room temperature it is easy for electrons to hop up to the empty levels and move under the impetus of an applied voltage (see Figure 1).

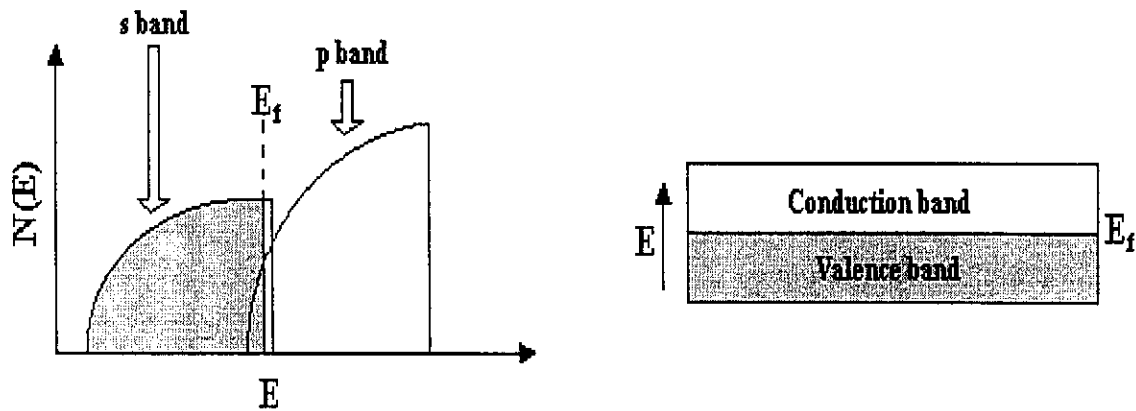


Figure 1: Band structure of a metal.

If, for a given solid, the conduction and valence bands are separated by a gap devoid of energy levels, called the bandgap, E_{bg} , then the solid is either a semiconductor or an insulator.

Insulators^{7, 8} have very small conductivities, and frequently their electrical characteristics are dominated by the presence of impurities (see Figure 2). A solid with a filled valence band and an energy gap to the next empty conduction band, will therefore be an insulator in its ground state. Very few electrons from the valence band have sufficient thermal energy to be promoted into the empty band above (i.e. the conduction band). Hence the conductivity is negligibly small.

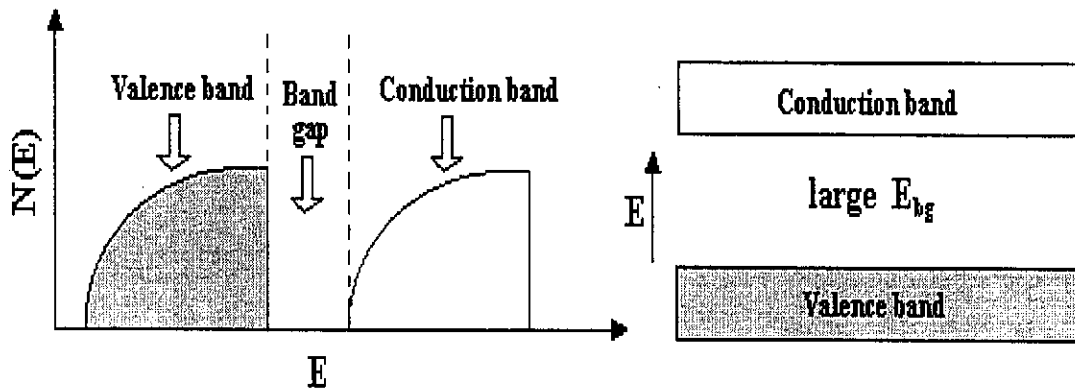


Figure 2: Band structure of an insulator.

The bandgap energy distinguishes semiconductors from insulators. Semiconductors have a similar band structure to insulators but the band gap is not very large: usually it is in the range 0.5eV to 3eV (see Figure 3), while insulator have bandgap energies larger than 3eV. Semiconductors fall into an intermediate region where the conductivity is small but increases in magnitude with increasing temperature. At least a few electrons have sufficient thermal energy to be promoted into the empty band.

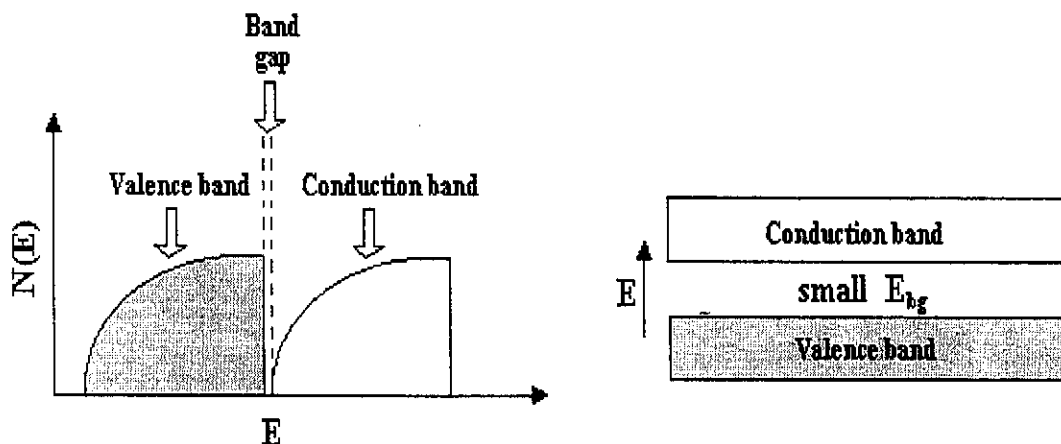


Figure 3: Illustration of a semiconductor, indicating the filled valence band and empty conduction band with a small energy gap.

Semiconductors^{7, 8} can be made conductive either by putting extra electrons into the conduction band or by removing electrons from the valence band. Consequently, there are two modes of conduction in a semiconductor. The first is the movement of electrons through the (mostly empty) conduction band. The second mode is electron flow in the valence band, but its description differs in solid state physics. Removal of an electron from the valence band creates a positively charged vacancy called a hole (see Figure 4). The hole can be regarded as the mobile entity because annihilation of a hole by a nearby electron effectively moves the hole over in space. So electrical current can be carried by either electrons in the conduction band or holes in the valence band, or by both types of charge carriers.

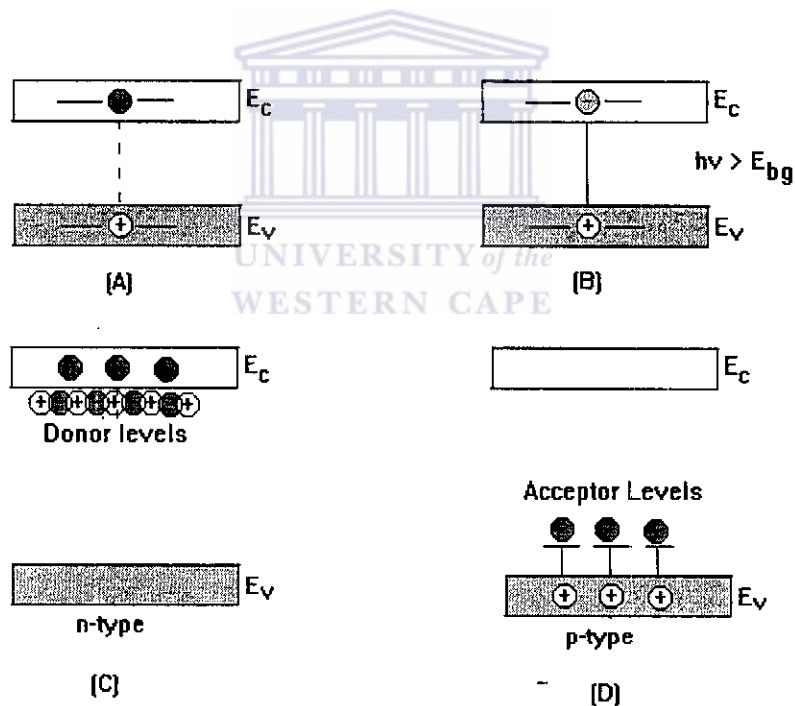


Figure 4: Mechanism of charge generation: (A) Thermal generation; (B) Photo-excitation; (C) Doping, n-type; (D) Doping, p-type.

Mobile charge carriers can be generated by three different mechanisms: thermal excitation, photo-excitation, and doping (see Figure 4). If the bandgap energy is sufficiently small, thermal excitation can promote an electron from the valence band to the conduction band. Both the electron and the accompanying hole are mobile.⁹

Semiconductors may be divided into two groups:

- (i) Intrinsic semiconductors are pure materials. The number of electrons, in the conduction band is governed entirely by the magnitude of the bandgap and temperature.
- (ii) Extrinsic semiconductors are materials whose conductivity is controlled by the addition of dopants.

Extrinsic semiconductors have much higher conductivities than similar intrinsic ones at normal temperatures.

In a similar manner, an electron can be promoted from the valence band to the conduction band upon the absorption of a photon of light (see Figure 4B). A necessary condition is that the photon energy exceeds the bandgap energy ($h\nu > E_{bg}$). This is the primary event in the conversion of sunlight to usable forms of energy. The bandgap energy therefore sets the condition for photon absorption. The semiconductor thus exhibits a threshold response to light.

The third mechanism of generating mobile charge carriers is doping.⁹ Doping is the process of introducing new energy levels into the bandgap. Doping can be effected by either disturbing the stoichiometry of the semiconductor (such as partially reducing a metal oxide) or by substituting a foreign element into the semiconductor lattice.

Two types of doping can be distinguished. For n-type doping, occupied donor levels are created very near the conduction band edge (see Figure 4C). Electrons from the donor levels are readily promoted to the conduction band by thermal excitation. Electrons in the conduction band outnumber the few thermally generated holes in the valence band, hence current is carried mainly by negative charge carriers.

Likewise, p-type doping corresponds to the formation of empty acceptor levels near the valence band edge (see Figure 4D). The acceptor levels trap electrons from the valence band, creating positive charge carriers. The donor and acceptor levels become charged due to loss or gain of electrons, but they are not charge carriers because they are fixed within the crystal lattice.

If the semiconductor remains intact and the charge transfer to the adsorbed species is continuous and exothermic the process is termed heterogeneous photocatalysis.¹⁰ Photochemical reactions that employ semiconductor powders as catalysts have received considerable attention because of the attractive possibility of solar energy conversion into stored chemical energy.¹¹ The solids used as photocatalysts are semiconductors with electrons as majority carriers.

The band gap absorption of photons leads to electrons and positive holes spatially separated by the surface potential in the space charge region, which increases their lifetimes, and make them available for the chemical reactions. Semiconductors are commonly described as n-type or p-type to indicate the dominant charge carrier; undoped semiconductors are referred to as intrinsic semiconductors. The band theory diagram for an n-type and a p-type impurity semiconductor is illustrated in Figure 5 and 6, respectively.

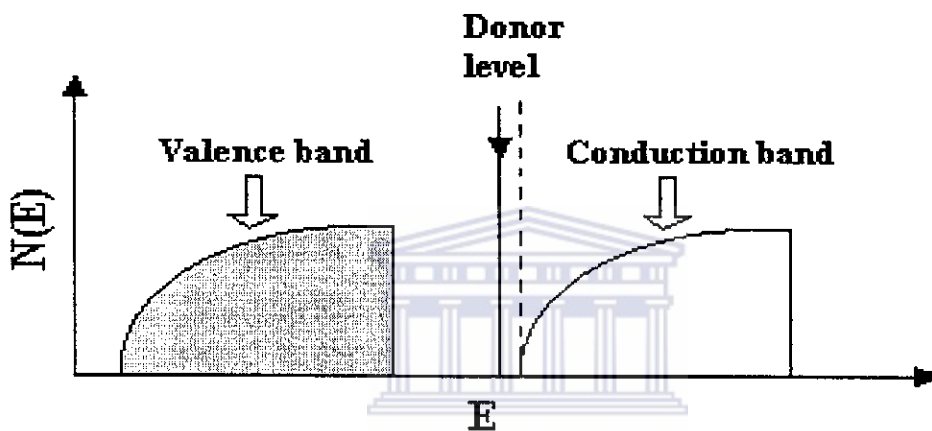


Figure 5: The band theory diagram for an n-type impurity semiconductor.

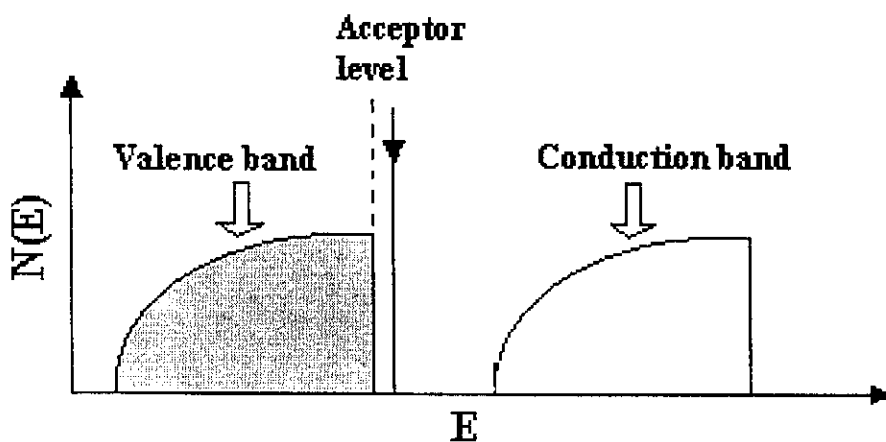


Figure 6: The band theory diagram for a p-type impurity semiconductor.

In an aqueous suspension, semiconductor particles behave as short-circuited microelectrodes under bandgap excitation and thus promote oxidation and reduction on the same particle.¹²

TiO₂ is an n-type semiconductor due to loss of oxygen (i.e. loss of O²⁻) this is accompanied by reduction of some Ti⁴⁺ to Ti³⁺.

For example, zinc oxide is metal oxide that also acts as an n-type semiconductor. Zinc oxide loses oxygen in heating in air. This is accompanied by the reduction of some zinc ions to atoms. Electrical conduction is due to the electrons associated with the zinc atoms, and since they are negative species zinc oxide is said to be an n-type semiconductor. In band theory terms, the zinc atoms constitute a donor level situated just below the bottom of vacant conduction band, so that excitation into the conduction band is relatively easy, and the conditions for electrical conduction are met (see Figure 5). Electrons attached to the zinc atoms are assigned to discrete energy level, because their concentration is low and they do not interact. The concentration of zinc atoms can also be increased through valence induction by doping with ions having a charge greater than 2+.

A wide range of other compounds - oxides, sulphides, etc. - with a variety of crystal structures is also semiconductors⁷ (see Table 1).

Table 1: Classification of semiconducting metal oxides.

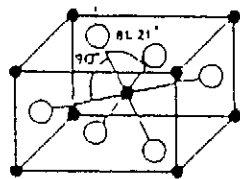
Effect of heating in air	Classification	Examples
Oxygen lost	Negative (n-type)	ZnO, Fe ₂ O ₃ , TiO ₂ , CdO, V ₂ O ₅ , CrO ₃ , CuO,
Oxygen gained	Positive (p-type)	NiO, CoO, SnO, Cu ₂ O, PbO, Cr ₂ O ₃

1.3 TiO₂ AS A PHOTOCATALYST

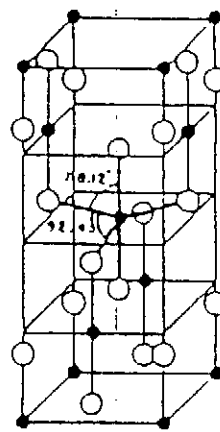
Probably the most well established example of semiconductor photocatalysis is paint chalking, which involves the photodegradation of the organic polymer part of the paint sensitized by the semiconductor pigment, usually TiO₂.¹³

The TiO₂ surfaces had been the subject of much study in recent years. TiO₂ is one of the semiconductor materials that can be found in rural as well as in urban atmospheres which is emitted from both natural and anthropogenic sources.¹⁴

Even after choosing TiO₂ as the semiconductor photocatalyst, the choice of which crystalline form is still important. Rutile and anatase are the two most common forms used TiO₂ (see Figure 7).



(A)



(B)

Figure 7: Structure of the TiO_2 (A) rutile and (B) anatase.

Anatase has always shown a photocatalytic activity much higher than that of rutile in all types of reaction media and in the presence of O_2 as an oxidizing species.¹⁵⁻²⁰ However, rutile has revealed a significant catalytic activity, comparable to that of anatase, in the presence of oxidants different from oxygen, such as Ag^+ or H_2O_2 .²¹ The different behavior of rutile and anatase, was initially attributed to the different position of the conduction band (more positive for rutile) and to the higher recombination velocity of electron-hole pairs photoproduced in rutile.^{15, 16}

Another explanation, in particular when O_2 is present, can be given by taking into account that O_2 has to be adsorbed over the TiO_2 surface before reduction and that the amount of O_2 that can be adsorbed depends on the hydroxylation degree of the adsorbing surface, and hence on the acid-base surface properties. These properties depend on the chemical history of TiO_2 , that is, on the preparation method and on the thermal treatment.²²

The surface of the TiO₂ anatase is in general very hydroxylated and can gradually lose water at the expense of surface hydroxyl groups under thermal treatment. The decrease of density of surface OH⁻ groups has already been correlated with the decrease of photocatalytic activity of TiO₂.^{23, 24} Rutile TiO₂, normally obtained at high temperatures, has a very low density of surface hydroxyl groups, and its rehydroxylation, even in contact with liquid water, is practically nil.²⁵⁻²⁷ From previous considerations, it seems that one of the fundamental reasons of the low photocatalytic activity of rutile is its poor adsorption capacity towards O₂.^{28, 29}

Recently,³⁰ by using the oxygen isotopic exchange (OIE) technique, a correlation has been proposed between the photocatalytic activity of rutile and anatase and their corresponding aptitudes toward oxygen exchange under irradiation. The higher photoactivity of anatase was correlated with its higher O₂ exchange ability.

Various titania samples of industrial origin (Degussa and Tioxide) have been characterized³¹ by electrical photoconductance measurements and tested as a function of their structure (anatase versus rutile). Anatase was constantly found more active than rutile, whatever the reaction chosen (mild oxidation of pure cyclohexane and 2-propanol; total degradation of phenol and nitrophenol isomers in water).

In identical conditions, Degussa³¹ was found more active, but the intrinsic activity, expressed in moles converted per hour and per square meter of active surface, was found slightly higher than Tioxide.

Exposure of TiO_2 to near UV-light causes the excitation of electrons from the valence band to the conduction band, generating pairs of reducing and oxidising centers. The oxidising centers are short-lived and trapped by surface $-\text{OH}^-$ groups to yield chemisorbed OH radicals, which terminate with the formation of molecular oxygen.³²

Electrons in the conduction band are trapped by metal ions in the lattice, giving rise to excited titanium ions in lower oxidation states at which the reduction of the substrates presumably can take place.³²

1.4 NITROGEN FIXATION

Air is a blend of O_2 , N_2 , CO_2 , H_2O vapor and small amounts of other gases. Nitrogen and its compounds play a key role in our economy. Of the "top 14" chemicals produced by industry in 1989, five contain nitrogen. See Figure 8 below.

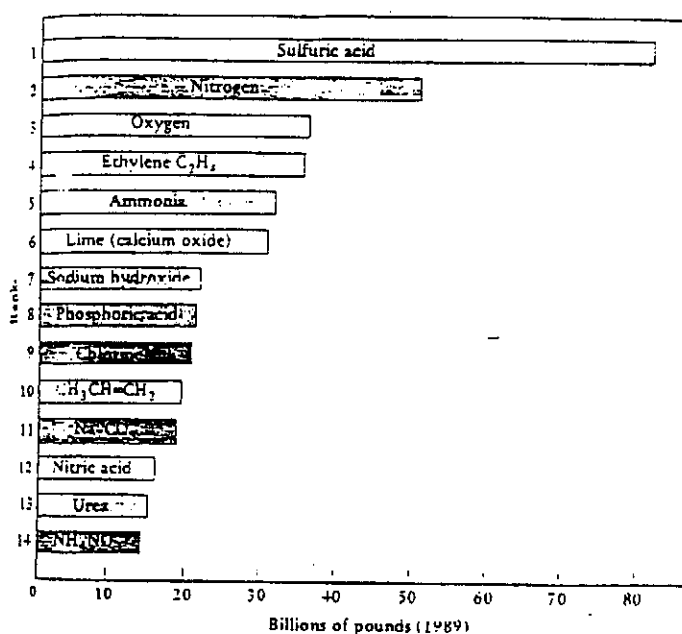


Figure 8: Indication of "top 14" chemicals produced by the industry.

More than 25% of the ammonia produced is used directly as a fertilizer, and the remainder is the starting material for other nitrogen-containing compounds. Either directly or indirectly, ammonia is the key to many industries: it goes into the starting materials for nylon production, household detergents, water purification, and the production of pharmaceuticals.

In a typical industrial plant, a mixture of air and 10% NH_3 is passed very rapidly over a catalyst at 5 atm pressure and $\sim 850^\circ\text{C}$. Roughly 96% of the ammonia is converted to NO_2 , making this one of the most efficient industrial catalytic reactions. The final step is to absorb the NO_2 into water to give the nitric acid and NO , the latter being recycled back into the process.⁵

Roughly 20% of the ammonia produced every year is converted to nitric acid, which in turn finds many uses. By far the greatest amount of the acid is turned into ammonium nitrate by neutralization of nitric acid with ammonia. Most of the NH_4NO_3 is consumed as fertilizer, but another use depends on the fact that it is thermally unstable and potentially explosive. A mixture of NH_4NO_3 and fuel oil is used as an explosive in mining operations.^{5, 33}

1.5 NITROGEN FIXATION IN NATURE

The world's growing population depends on supplies of nutrients, especially nitrogen compounds, in the soil. Plants need minerals to grow and the concentration of nitrate and ammonium ions in the soil often limits crop growth. Even though we are bathed in tons of nitrogen gas, plants cannot use it until it is "fixed", converted into biologically useful forms such as nitrates and ammonia. Thus the process by which atmospheric nitrogen is incorporated into nitrogen compounds that can be utilized by plants is known as nitrogen fixation.^{34, 35, 37}

On a worldwide basis, most nitrogen fixation is carried out by a few types of microorganisms, including both free-living and symbiotic forms of cyanobacteria and heterotrophic bacteria. Of the various classes of nitrogen-fixing organisms, the symbiotic bacteria are by far the most important in terms of total amounts of nitrogen fixed. The most common of the nitrogen-fixing symbiotic bacteria is *Rhizobium*, which invades the roots of leguminous plants, such as clover, peas, beans, vetches, and alfalfa.^{34, 36}

Where leguminous plants are grown, some of the "extra" nitrogen may be released into the soil. The leguminous plants are then either harvested, leaving behind the nitrogen - rich roots, or, better still, plowed back into the field. Much of the nitrogen found in the soil is the result of the decomposition of organic materials and so is in the form of complex organic compounds, such as proteins, amino acids, nucleic acids, and nucleotides it then becomes available to other plants.

The process by which this limited amount of nitrogen is circulated and recirculated throughout the world of living organisms is known as the nitrogen cycle.³⁴⁻³⁶ As Figure 9 shows, the movement of nitrogen from the atmospheric reservoir, through organisms, then back to the atmosphere involves six processes: nitrogen fixation, assimilation and biosynthesis, decomposition, ammonification, nitrification, and denitrification.

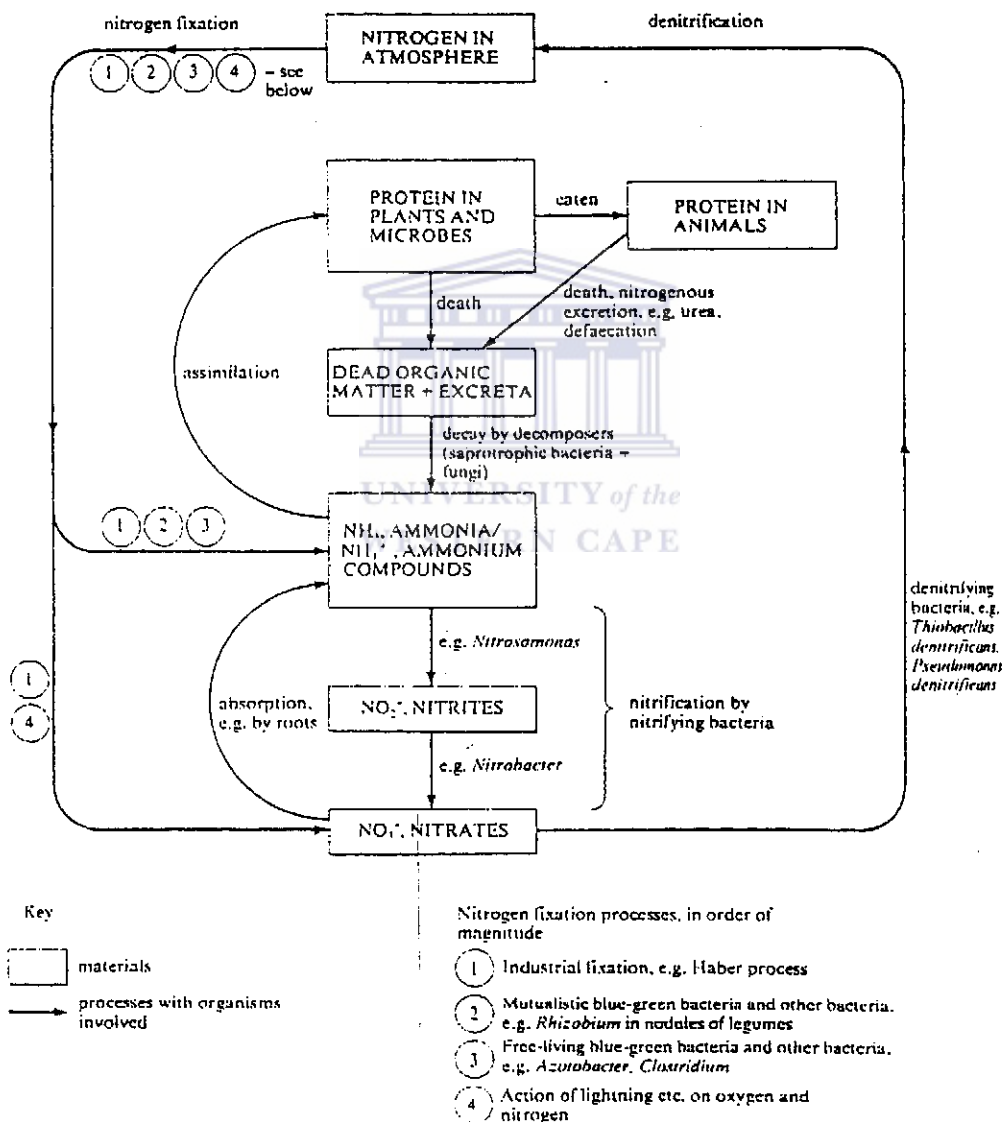


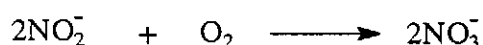
Figure 9: Nitrogen cycle

In nitrogen fixation certain soil bacteria take up nitrogen from the air. They attach electrons (and associated H ions) to the nitrogen through a series of reactions, thereby forming ammonia (NH₃) or ammonium (NH₄⁺). They use these compounds in growth, maintenance, and reproduction.

When the nitrogen-fixing microbes die, the compounds are released during decay processes. Other bacteria present in soil use the compounds as energy sources. When ammonia and nitrate dissolve in soil water, they can be assimilated by plant root and incorporated into organic compounds. These organic compounds are the only nitrogen source for animals, which feed directly or indirectly on plants.

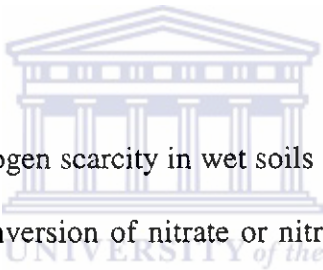
Later, in a process called ammonification,³⁴⁻³⁶ the nitrogen-containing wastes and remains of plants and animals are decomposed by some species of bacteria and fungi. The decomposers use some nitrogen for their own growth, and they release the excess as ammonia or ammonium. Plants then reuse some of these nitrogen-containing by-products.

In nitrification, soil bacteria strip the ammonia or ammonium of electrons, and nitrite (NO₂⁻) is released as a product of the reaction. Still other nitrifying bacteria then use nitrite for energy metabolism, which yields nitrate (NO₃⁻) as a product.



Nitrogen is often the limiting nutrient for plant growth. Some plants, however, benefit from increased rates of nitrogen uptake because of a mutually beneficial interaction with free-living or symbiotic microorganisms. Legumes (such as peas and beans) are an example. They harbor nitrogen fixers in nodules in their roots, supplying their guests with energy-rich sugar molecules in exchange for fixed nitrogen.³⁶

In itself, the continual production of ammonia by innumerable bacterial populations would seem to assure plants of plenty of nitrogen. Yet soil nitrogen is scarce. During crop harvests, of course, some nitrogen leaves the fields with the plants. Because nitrite, nitrate, and ammonia are soluble, some may run off in streams and rainwater.^{36, 37}



However, the major cause of nitrogen scarcity in wet soils is a bacterial process called denitrification^{34, 36} that is the conversion of nitrate or nitrite to N_2 and nitrous oxide (N_2O). The overwhelming majority of bacteria that take part in this process are ordinary species that rely on aerobic respiration. Under some conditions, through, especially when soil is poorly aerated, they switch to anaerobic electron transport. They use nitrate, nitrite, or nitrous oxide instead of oxygen as the terminal electron acceptor.

1.5.1 Nitrogen in Agriculture

With any loss of fixed nitrogen, soil fertility (hence plant growth) is reduced. Farms in Europe and in North America have depended on crop rotation to restore the soil. For example, legumes are planted between plantings wheat or sugar beet crops.

This practice has helped maintain soils in stable and productive condition, in some cases for thousands of years. Modern agriculture,^{36, 37} however, depends on nitrogen-rich fertilizers. To overcome the lack of nitrate in the soil, farmers add extra nitrate in the form of inorganic fertilizers. With plant breeding, fertilization, and pest control, the crop yields per acre have doubled and even quadrupled over the past forty years.

With intelligent management, it appears that soil can maintain such high yields indefinitely - as long as water and commercial nitrogen-containing fertilizers are available. The catch, of course, is that enormous amounts of energy are needed to produce fertilizer - not energy from the unending stream of sunlight, but energy from petroleum. As long as the supply of oil was viewed as unending, there was little concern about the energetic cost of fertilizer production.

In many cases, we have been pouring more energy into the soil (in the form of fertilizer) than we are getting out of it (in the form of food). Unlike natural ecosystems, in which nutrients such as nitrogen are cycled, our agricultural systems exist only because of constant, massive infusions of energetically expensive fertilizers.^{36, 37}

As long as the human population continues to grow exponentially, farmers will be engaged in a constant race to supply food to as many individuals as possible. Soil enrichment with nitrogen-containing fertilizers is essential in the race.

1.6 NITROGEN FIXATION AS AN INDUSTRIAL PROCESS

Nitrogen fixation is also carried out industrially, with the required energy supplied by fossil fuels. As the cost of these fuels increases, so does the price of the nitrogen-containing fertilizer produced. At present, the equivalent of two million barrels of oil a day is required for the production of nitrogen -containing fertilizers. In this perspective, investigation of the mechanism of nitrogen fixation by microorganisms takes on great practical significance.³⁴ Crops rapidly consume available nitrogen in soils, and chemical fertilisers, prepared industrially by taking nitrogen from the atmosphere make up the shortfall.³⁸

Food production depends primarily on plants finding adequate amounts of nitrogen compounds in the soil. Nitrogen fixation comes into the question because, though farmers can supply more than 80% of the necessary nitrogen compounds by recycling nitrogen already in the biosphere (as composts, organic manures and such), there is wastage. The nitrogen cycle shows that, on a global scale, soil nitrogen had at present to be topped up with about 12% new nitrogen each year.^{38, 39}

The only important source of such nitrogen is the atmosphere. Nitrogen fixation is the conversion of atmospheric nitrogen into forms that plants can use, a conversion principally performed by nitrogen-fixing bacteria or by industrial chemists using the Haber process. The most important industrial method for ammonia production is the Haber process.

If nitrogen and hydrogen are heated together, a reversible reaction takes place, yielding a small percentage of ammonia. At the outset, this seems a poor choice for several reasons. Hydrogen is available naturally only in combined form in water or hydrocarbons, for example. This means that some H-containing compounds must be destroyed first at the cost of considerable energy. Not only that, the energy expense is completely wasted because the hydrogen of ammonia is converted to water and the nitrogen to nitrate by soil bacteria before ammonia can be taken up by the plants.

The plant must then expend more energy, derived from photosynthesis, to reduce the nitrate back to ammonia.^{5, 35} The reaction at ordinary temperatures is so slow as to be useless. It will be noticed that the reaction is exothermic. Hence, according to Le Chatelier's Law, an increase of temperature will reduce the yield of ammonia, and use of a catalyst may increase the speed of the reaction until a reasonable time.

A German chemist, Fritz Haber (1868 - 1934), worked out the exact conditions for commercial exploitation of this process. Large scale production began in Germany in 1913. Prior to this discovery Germany was dependent chiefly on nitrate from Chile for her explosive and fertilizer raw materials. With the development of the Haber process, Germany was able to use the inexhaustible source of nitrogen in the atmosphere.²

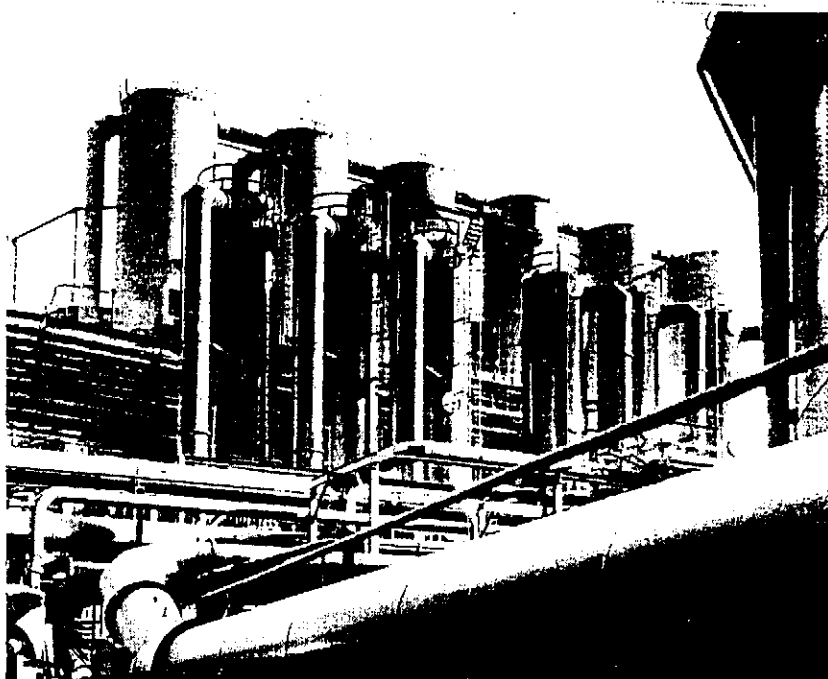
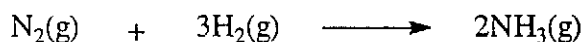


Figure 10: Part of the plant used in the synthesis of ammonia.

The Haber process consists of compressing a mixture of hydrogen and nitrogen to several hundred times of atmospheric pressure, in the presence of a catalyst. The temperature may be raised to about 500°C, in order to achieve an acceptable reaction rate. Increasing the temperature renders the production of NH₃ less thermodynamically favorable, but operating at high pressure (150-350 atm) can offset this advantage. It takes energy equivalent to 400 tons of coal to produce a single ton of NH₃ by the Haber processes, and a typical plant produces up to 1650 tons of NH₃ per day. See Figure 10 above.



The catalyst is iron to which small amounts of potassium and aluminum oxides have been added. These added substances greatly increase the activity of the iron catalyst.⁴⁰

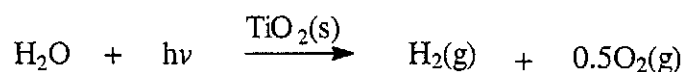
The equilibrium mixture of nitrogen, hydrogen and ammonia is removed from the catalyst, the ammonia taken out of the mixture, and the remaining gases are recirculated back to the catalyst chamber. The process requires a large supply of pure nitrogen and pure hydrogen. The former is obtained through the liquifaction of air, the latter either by the water-gas reaction, the steam-hydrocarbon reaction, or by electrolysis. Purification of these gases is often a major expense in the process.

There are several other methods for the industrial production of ammonia. One of these is the utilization of by-product ammonia given off during the manufacture of coal gas and coke from coal.²

1.7 PHOTOCATALYTIC REACTIONS USING TiO₂ AS A PHOTOCATALYST



The band-gap of TiO₂ is in order of 2.9 - 3.2eV, corresponding to the energy of near UV light of wavelength between 390-420nm. The gap is sufficiently large to provide energy for the water splitting reaction, which,



after its discovery by Fujishima^{34, 35} et al is still being extensively studied for potential applications in solar energy conversion systems.

This event marked the beginning of a new era in heterogeneous photocatalysis. Since then, research efforts in understanding the photocatalytic efficiency of TiO₂ have come from extensive research performed by chemists, chemical engineers and physicists. In recent years, applications to environmental cleanup have been one of the most active areas of research in heterogeneous photocatalysis. This is inspired by the total destruction of organic compounds in polluted air and wastewaters.¹⁰

Inoue⁴¹ et al first reported that a suspension of TiO₂ photocatalyzes the reduction of CO₂ with water to produce formic acid, formaldehyde, methanol, and a trace amount of methane. Studies by Hirano⁴² et al observed methanol as the main photoreduction product from CO₂ when a Cu-containing TiO₂ suspension was irradiated.

Several researchers have designed experiments to enhance the efficiency and selectivity for CO₂ photoreduction. Ishintani⁴³ et al systematically investigated the effect of different metals on the TiO₂ catalysts. The Pd-TiO₂ system exhibited very high selectivity for the production of methane from CO₂ photoreduction.

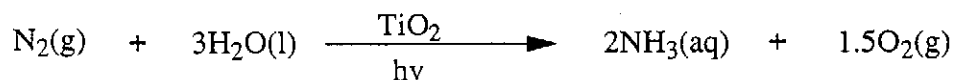
Photofixation of dinitrogen on irradiated semiconductor surfaces is an attractive way of solar energy conversion.³⁵ Several TiO₂-based catalysts produce ammonia upon irradiation with UV light in a stream of N₂. Solids,⁴⁴ wafers⁴⁵ and suspensions⁴⁶ have been employed. The yields in all cases are small and the activity decreases with time.⁴⁶

The fixation of atmospheric dinitrogen by means of its conversion to more reactive species as NH_3 , NO_3^- , etc., has attracted the attention of several researchers.³³ Next to biological photosynthesis, a recent new route for fixing atmospheric dinitrogen, involving illuminated inorganic semiconductor materials has been developed since the heterogeneous photocatalytic production of ammonia from N_2 on wet titania and iron-doped titania catalysts, was described by Schrauzer⁴⁴ et al.

Adsorbed water was photodecomposed to yield oxygen, and at the same time nitrogen was reduced to produce NH_3 and N_2H_4 . The hydrogenation of unsaturated hydrocarbons was also achieved photocatalytically in the same study.⁴⁴

1.8 NITROGEN FIXATION USING PHOTOCATALYSIS

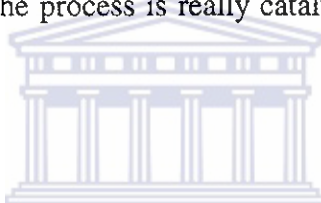
A possible alternative method for synthesizing ammonia is the photofixation of dinitrogen on irradiated semiconductor surfaces. Atmospheric dinitrogen has been reported to be fixed on titanium photocatalysts in two ways either by reduction⁴⁴ of N_2 to NH_3 or by oxidation^{47, 48} of N_2 to $\text{N}_2\text{O}_2^{2-}$. The prospect of a photocatalytic synthesis of NH_3 from N_2 and H_2O with sunlight, was first described by Schrauzer et al.⁴⁴



The ΔG° for the reaction above is 678kJ/mol. This reaction is endergonic, thus requiring an input of energy. Very low yields were obtained.

Schrauzer⁴⁴ et al reported that the rate of ammonia increased linearly with increasing nitrogen pressure up to about 0.6 atm, then more slowly to a maximum at about 1.5 atm. They also reported that virtually no hydrogen was formed when the most active catalysts were irradiated at low temperatures (30-50°C). The claim that NH₃ can be synthesized catalytically from nitrogen and water in the presence of simple oxide based semiconductors suggests a process of overwhelming importance.

Hence, it is enticing for many researchers to conduct a large number of experiments with various semiconductor catalysts but they appear to produce very small yields of NH₃. No significant breakthrough has been achieved in enhancing the yield of ammonia; the question whether the process is really catalytic or not seems to be still not answered.⁴⁹



Photoreduction of N₂ to NH₃ on Ru-doped rutile has been reported.⁵⁰ Ilperuma⁵¹ et al discovered that NO₃⁻ is observed in higher yields than NH₃. TiO₂ catalysts coated with Ag, Hg and Pt appear to produce predominately NH₃ while ZnO produce only nitrate.

Though it has been demonstrated that the reduction of dinitrogen is feasible at ordinary temperatures and pressures in the presence of light and a catalyst, the low yields of NH₃ obtained thus far seem to point out that such a process cannot compete with the well established Haber process. The photocatalytic route has been successful only to the extent of producing a few molecules of NH₃.⁵²

Although many studies of N₂ photoreduction on semiconductors have been reported in literature, oxidation is predominant on illuminated TiO₂ surfaces. The ability of TiO₂ surfaces to fix dinitrogen oxidatively has been investigated by Bickley et al.^{47, 53,}

54

1.9 PHOTOCATALYTIC OXIDATIVE NITROGEN FIXATION

In 1979 Bickley⁴⁷ et al reported some results in which nitrogen has been fixed on the surface of rutile TiO₂ by low energy UV photons, at room temperature in oxidising conditions. They proposed a photocatalytic nitrogen fixing mechanism that is discussed in this section.

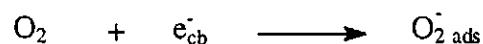
When TiO₂ which adsorbed water, show significantly greater photochemical reactivity towards O₂ than specimens which have been dehydroxylated.



Adsorbed hydroxyl groups, OH⁻ act as traps for the positive holes, h_{vb}⁺, which is in the valence band of TiO₂.

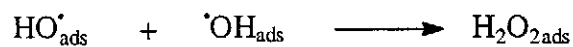


The hole trapping leaves the conduction band electron available to interact with the ambient atmosphere and the chemisorption of molecular oxygen takes place according to:



The adsorbed species O_2^- have been identified but the hydroxyl radicals, OH^\cdot , were difficult to confirm.

A comparison was made with TiO_2 surface, which contained pre-adsorbed H_2O_2 only; H_2O_2 is formed on the surface of TiO_2 during the irradiation, probably through the direct interaction of the hydroxyl radicals, which form during the hole trapping process.



The TiO_2 surface which consists of pre-adsorbed H_2O_2 are irradiated in pure oxygen, O_2 , whereas it seems that the nitric oxide forms directly if the irradiation takes place in air or a nitrogen-oxygen mixture. Thus the molecular nitrogen can be fixed at the surface of the TiO_2 through its interaction with the H_2O_2 .

Hence, Bickley⁴⁷ et al suggested that the adsorbed species from which the gaseous nitric oxide originates is probably adsorbed of molecular nitric oxide, or one of its ions, and its proposed reaction:



The X-ray photoelectron spectroscopic (XPS) examinations of the surfaces of these TiO_2 specimens show nitrogen signals at a binding energy of 399.5eV, confirming the presence of an adsorbed species containing nitrogen.

Electron paramagnetic resonance studies of the samples containing the fixed nitrogen failed to detect any species which could be ascribed to adsorbed molecular nitric oxide. They concluded that the adsorbed species is probably NO_{ads}^- (or $\text{N}_2\text{O}_2^-_{\text{ads}}$).

Due to the above mentioned report Schrauzer³² et al continued this experiment and detected the formation of traces of nitrites but not nitrates at the liquid-solid interface, from the aqueous extracts of TiO_2^- after their exposure in air to UV illumination.

From the results reported in the literature it is inferred that there are some doubts about the mechanism for the heterogeneous photofixation of nitrogen on inorganic semiconductor materials; in particular the identity of the nitrogen-containing species, photo-oxidatively fixed on TiO_2 remains unclear.

In an attempt to identify the surface nitrogen species on the basis of the previously possibilities, e.g. $\text{N}_2\text{O}_2^{2-}$. Navio⁴⁸ et al demonstrated that principal species formed during the photo-oxidative fixation of molecular nitrogen on TiO_2 is hyponitrite, $\text{N}_2\text{O}_2^{2-}$ anion.

Chapter 2



2.1 AIM

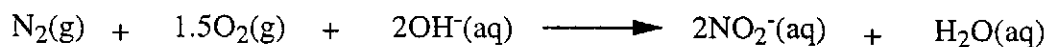
The aim of these studies is to oxidatively fix dinitrogen by photocatalysis.

2.2 BACKGROUND THEORY

The report by Navio⁴⁸ et al in 1994, (mentioned in section 1.9) confirmed fixation of dinitrogen on the TiO₂ photocatalyst. The hyponitrite species is not a stable anion thus this species may undergo further oxidation to more stable species such as nitrate, NO₃⁻ and nitrite, NO₂⁻.⁵⁵

The following theory is proposed here to justify the approach of attempting to photocatalytically fix dinitrogen oxidatively on a TiO₂ photocatalyst. The proposed mechanism shows that photooxidation of N₂ is much more promising than that of photoreduction.

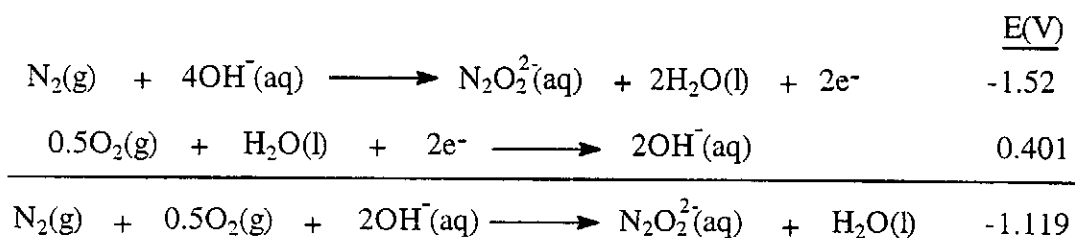
Consider:



at pH = 7, $\Delta G^\circ = 89\text{kJ/mol}$ of N₂ and at pH = 14, $\Delta G^\circ = 7\text{kJ/mol}$ of N₂

The above reaction is much more thermodynamically feasible than reduction to NH₃, however once again N₂ would not be oxidised to NO₂⁻ in a single electron step.

Now at pH = 14



The energy level diagram of TiO_2 is represented in Figure 11 below, which shows that when TiO_2 is exposed to appropriate light irradiation in air O_2 could be reduced to OH^- and N_2 oxidised to $\text{N}_2\text{O}_2^{2-}$.

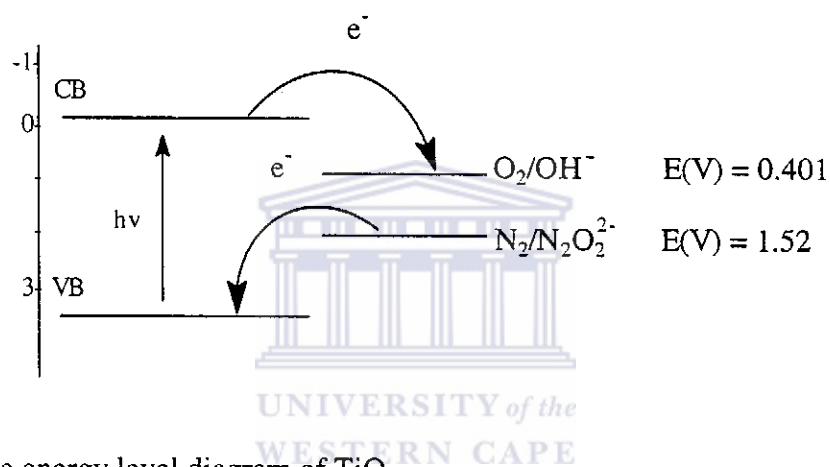
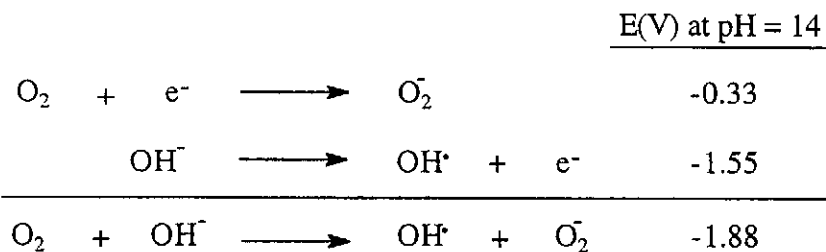
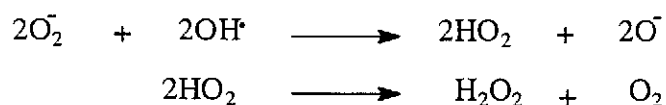


Figure 11: The energy level diagram of TiO_2 .

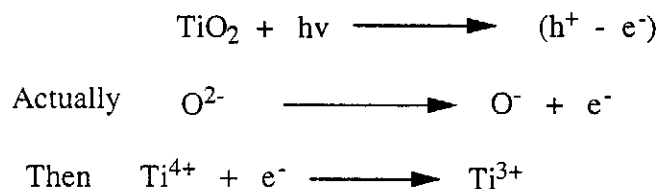
But in practice neither of the above half reactions is likely because it is established that photo absorption of O_2 and chemisorption of OH^- causes the following on TiO_2 .²⁸



Then

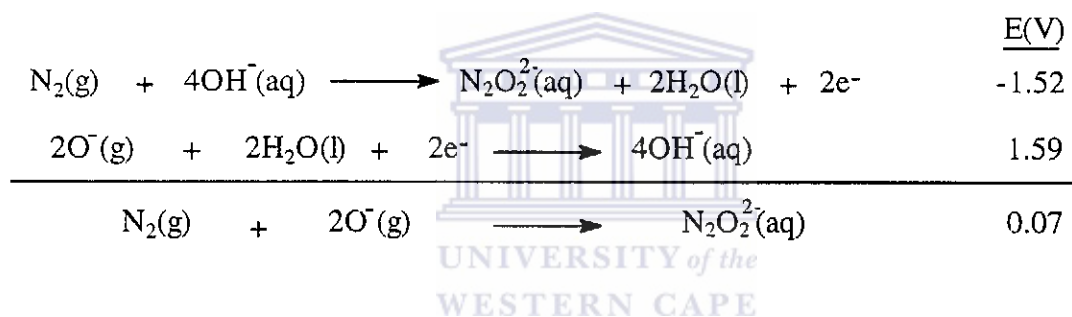


Exciton formation on irradiation if TiO₂ also forms O[•]



O[•] is a powerful oxidising agent that can spontaneously oxidise N₂ to N₂O₂²⁻. So the bandgap of TiO₂ is required but only to form O[•].

Now at pH = 14

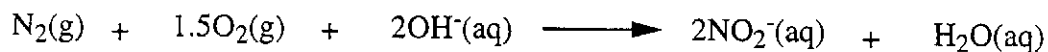


Hence ΔG is negative, and the reaction spontaneous. This species may then undergo further oxidation to more stable species such as nitrite, NO₂⁻ and then nitrate, NO₃⁻.

But N₂ does not chemisorb on TiO₂ but does when TiO₂ is treated with H₂O₂.⁴⁷ Thus irradiation of N₂ and O₂ in the presence of peroxide treated TiO₂ at pH = 14 should be appropriate conditions to attempt the photooxidation of N₂.

Thus our particular interest is the possibility of photocatalytic oxidation of dinitrogen in alkaline solution containing suspensions of photocatalysts.

The reaction involved at pH 14.



The ΔG° for the overall reaction above is 7kJ/mol of N_2 .

In this preliminary study the two photocatalysts will be prepared that is titanium peroxide compounds and titanium dioxide, TiO_2 pretreated with hydrogen peroxide, H_2O_2 . Aqueous suspensions of these photocatalysts will then be exposed to irradiation in air.

The presence of any nitrogen species such as, nitrate, NO_3^- and nitrite, NO_2^- in the aqueous extracts will then be investigated.

The potential photocatalysts will be investigated at different irradiation times, pH, mass of photocatalysts in the suspension, concentration of H_2O_2 in the suspension and wavelength of irradiation used.

After establishing optimum conditions for oxidative fixation, these conditions will be employed to investigate whether samples of RBM rutile are active as photocatalysts. Richards Bay Minerals (RBM) mine titanium bearing sands in South Africa and we are interested in the potential of their products to fix nitrogen.

Chapter 3

EXPERIMENTAL



UNIVERSITY *of the*
WESTERN CAPE

3.1 MATERIALS USED

- A. The titanium (IV) isopropoxide 97%, $\text{Ti}[\text{OCH}(\text{CH}_3)_2]_4$ was purchased from the Aldrich Chemical Company.
- B. The Degussa Company provided Degussa P25 (75% anatase and 25% rutile) TiO_2 .
- C. Titanium oxysulphate-sulphuric acid complex hydrate, $\text{TiOSO}_4 \cdot x\text{H}_2\text{SO}_4 \cdot x\text{H}_2\text{O}$ purchased from the Aldrich Chemical Company.
- D. The RBM rutile flour (200mesh, 75micron) and the concentrated rutile were manufactured by Richard Bay Mineral, RBM.
- E. All solvents used were AR grade. All dilutions were made with distilled water.

3.2 CATALYST PREPARATION

3.2.1 Preparation of titanium peroxide compounds.

Method I (after Connor⁵⁶ et al)

In a typical experiment 0.5g of titanium oxysulphate-sulphuric acid complex hydrate, $\text{TiOSO}_4 \cdot x\text{H}_2\text{SO}_4 \cdot x\text{H}_2\text{O}$, was weighed and suspended in 20ml of distilled water. All the $\text{TiOSO}_4 \cdot x\text{H}_2\text{SO}_4 \cdot x\text{H}_2\text{O}$ dissolved after several minutes. 20ml of 20% hydrogen peroxide, H_2O_2 and ethanol was added. A red solution was obtained. The pH was adjusted to 14 using sodium hydroxide, NaOH. A yellow precipitate formed on standing at room temperature. The precipitate was then filtered, washed with distilled water and dried at room temperature. The product was then weighed and a very low yield was obtained. The solid was then transferred to the irradiation reactor for further use.

Method II (after Jere⁵⁷ et al)

In a typical experiment the titanium hydroxide was prepared by hydrolysis of titanium (IV) isopropoxide. 10ml of distilled water was poured into a beaker that was stirred vigorously while 2ml of titanium (IV) isopropoxide were added dropwise to the water. A white precipitate of the titanium hydroxide formed. The titanium hydroxide was dried and weighed, then suspended in water. 0.5g of titanium hydroxide was weighed and suspended in 20ml of distilled water. The mixture was vigorously stirred with addition of 10ml of 20% H₂O₂, until the titanium hydroxide dissolved. A yellow solution was obtained and left to stand. A yellowish colloid formed after which the pH was adjusted with 1M NaOH or 1M H₂SO₄. The colloidal suspension was then used directly in the experiments.

Due to the gel formation of these particular compounds the removal of the excess H₂O₂ was extremely difficult.



Several studies^{57, 66-70} show differences in the formulae and structures of the peroxo complexes of titanium. It may be that many of the researchers worked at different pH-values. Studies show that when the pH values are adjusted the structure and formulae of the peroxo complexes changes. As several studies have made clear,^{58, 58} the colour of an aqueous solution of Ti(IV) in H₂O₂ depends on the pH, being orange in acid solutions, yellow in solutions of about pH 8, and colourless in strongly alkaline solutions.⁵⁶

3.2.2 Preparation of H₂O₂ treated Degussa P25, TiO₂

In a typical experiment 0.5g of TiO₂ was suspended in 20ml of water, followed by the addition of 20ml of 1M NaOH and 20ml of 20% hydrogen peroxide, H₂O₂. A yellow suspension was obtained. The pH was adjusted using 1M NaOH or 1M H₂SO₄. The mixture was heated at 70°C for about 40-45 minutes before use.

The TiO₂ treated with H₂O₂ was the other catalyst used as was described by Schwarz⁵⁸ et al. In the experiment described by Schwarz⁵⁸ et al the H₂O₂ and TiO₂ are added to a hot alkaline solution obtaining a yellow colour, which was characterised as peroxy species.

3.2.3 Preparation of H₂O₂ treated RBM rutile flour

Rutile flour was suspended in water and heated for an hour. The hot suspension was filtered off, washed with water then dried in an oven. Rutile flour was suspended in water, followed by the addition of 1M NaOH and hydrogen peroxide, H₂O₂. The pH was adjusted using 1M NaOH and 1M H₂SO₄. The mixture was heated at 70°C for about 40-45 minutes before use.

3.2.4 Preparation of H₂O₂ treated RBM concentrated rutile

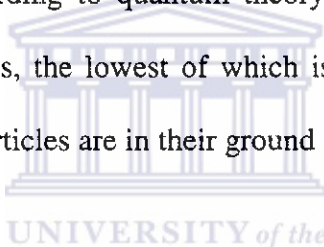
Concentrated rutile was suspended in water and heated for an hour. The hot suspension was filtered off, washed with water then dried in an oven. Concentrated rutile was suspended in water, followed by the addition of 1M NaOH and hydrogen peroxide, H₂O₂. The pH was adjusted using 1M NaOH and 1M H₂SO₄. The mixture was heated at 70°C for about 40-45 minutes before use.

The samples were characterised by using different analytical techniques such as FTIR, Vis/UV spectroscopy and SEM. (see section 3.3 for details).

3.3 CATALYST CHARACTERISATION

3.3.1 General uses of molecular spectroscopy⁵⁹

Molecular spectroscopy based upon ultraviolet, visible, and infrared radiation is widely used for the identification and determination of myriad inorganic and organic species. The spectroscopic nomenclature, absorption is a process in which a chemical species in a transparent medium selectively attenuates certain frequencies of electromagnetic radiation. According to quantum theory, every elementary particle has a unique set of energy states, the lowest of which is the ground state; at room temperature, most elementary particles are in their ground state.

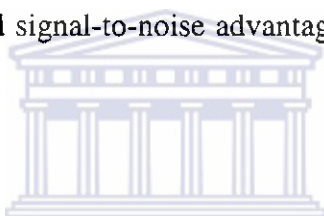


3.3.2 Fourier Transform Infra-red Spectroscopy (FTIR)⁵⁹⁻⁶¹

Infrared spectroscopy is a widely used industrial tool for the structural and compositional analysis of organic, inorganic or polymeric samples and for quality control of raw materials and commercial products. It is relatively simple technique, non-destructive, versatile enough to handle solids, liquids and gases with a minimum of sample preparation, and accurate enough for both the qualitative identification of the structure of unknown materials and the quantitative measurement of the components in a complex mixture. But in spite of all these benefits, infrared spectroscopy has certain drawbacks, which become more critical as the difficulty of the analytical problem increases.

These drawbacks stem from the fact that infrared is an energy-limited technique. The energy distribution of the blackbody radiation of the IR source reaches a peak in the low wavelengths. However, situations frequently occur where there is not enough energy to accurately measure very weak or very strong bands necessary for an analysis.

The applications of infrared spectroscopy today have experienced an explosive transformation with the introduction of interferometric methods of obtaining infrared spectra and the subsequent mathematical processing of the interferogram via vast Fourier transform algorithms to recover the frequency spectrum. The transformation has given us impressive time and signal-to-noise advantages, as well as a whole new generation of instrumentation.



Most multiplex instruments depend upon the Fourier transform for signal decoding and are consequently often called Fourier transform instruments. Fourier transform spectroscopy was first developed by astronomers in the early 1950s in order to study the infrared spectra of distant stars. Some of the special advantages of Fourier Transform Infrared spectroscopy are given in Table 2.

Table 2: Special advantages of FTIR spectroscopy.

Energy Limited Situations

Opaque samples < 1% Transmission

IR Emission studies

Very high resolution requirements

Time Limited Situations

Kinetic studies

Unstable compounds

Reaction of catalytic intermediates

Signal / Noise Limited Situations

Trace Analysis

Interfering Absorption

Atmospheric Sampling



The infrared region of the spectrum encompasses radiation with wavenumbers ranging from about 12,800 to 10 cm^{-1} or wavelengths from 0.78 to 1000 μm^{-1} . From the standpoint of both application and instrumentation, the infrared spectrum is conveniently divided into near-, mid-, and far-infrared radiation. To date the majority of analytical applications have been confined to a portion of the mid-infrared region extending from 4000 to 400 cm^{-1} (2.5 to 25 μm). The single most important use has been for the identification of organic compounds whose mid-infrared spectra are generally complex and provide numerous maxima and minima that are useful for comparison purposes.

The Perkin-Elmer diffuse reflectance⁶² (PEDR) accessory, gives you a convenient and sensitive method for analyzing a variety of solid samples. The Perkin Elmer diffuse reflectance (PEDR) accessory can be used with both Fourier transform and dispersive infrared spectrometers. The acronyms DRIFTS (Diffuse Reflectance using Infrared Fourier Transform Spectrometry.) and DRUIDS (Diffuse Reflectance Using Infrared Dispersive Spectrometry) denote these two techniques.

The diffuse reflectance method provides the following advantages:

- (i) convenient and rapid sample preparation, involving grinding to powder form or roughing the surface of a solid material;
- (ii) a wide variety of solid sample forms, including powdered, cast from solution, or dispersed on carborundum paper;
- (iii) high sensitivity, making the method convenient for microsampling;
- (iv) no polymorphic changes in crystalline structure, if the sample is not ground.

Methods and Instrument used

Solids were recorded using DRIFTS in KBr. The following procedure was used for characterisation of the titanium peroxide compounds. The sample was carefully ground and mixed with fine KBr. The mixture was then placed into the sample cup and tapped on the bench top to level the top surface of the sample. The cup was placed into the cup holder of the instrument (Figure 12). The spectrum was obtained using a Perkin Elmer Paragon 1000PC FTIR spectrophotometer.

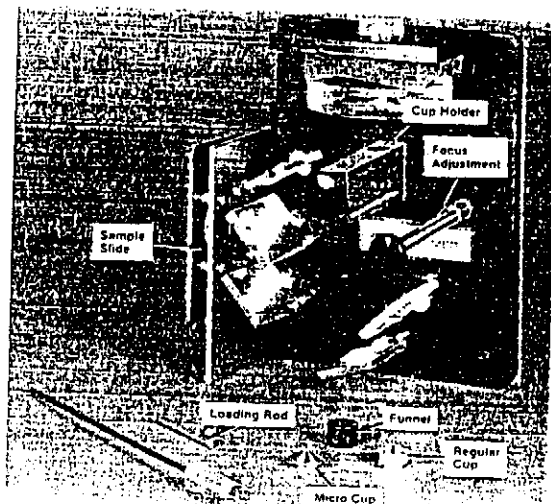


Figure 12: The Perkin-Elmer Diffuse Reflectance Accessory

3.3.3 Scanning electron microscopy (SEM) ^{61, 62}

SEM is used in many fields i.e. chemistry, material science, geology, and biology. The use of the SEM is employed to characterise the surfaces of solids on a submicrometer scale. A detailed knowledge of the physical nature and chemical composition is obtained. SEM provides morphology and topographic information about the surfaces of solids that is usually necessary in understanding the behaviour of surfaces.

The scanning electron microprobe furnishes qualitative and quantitative information about the elemental composition of various areas of a surface. All electron microscopes have an electron gun, a system of condenser lenses, and some sort of signal detector. The SEM needs scanning coils and an electron detector. The SEM becomes a microprobe analyser (EPMA) when an X-ray detector is added or a STEM when the detector is moved below the specimen.

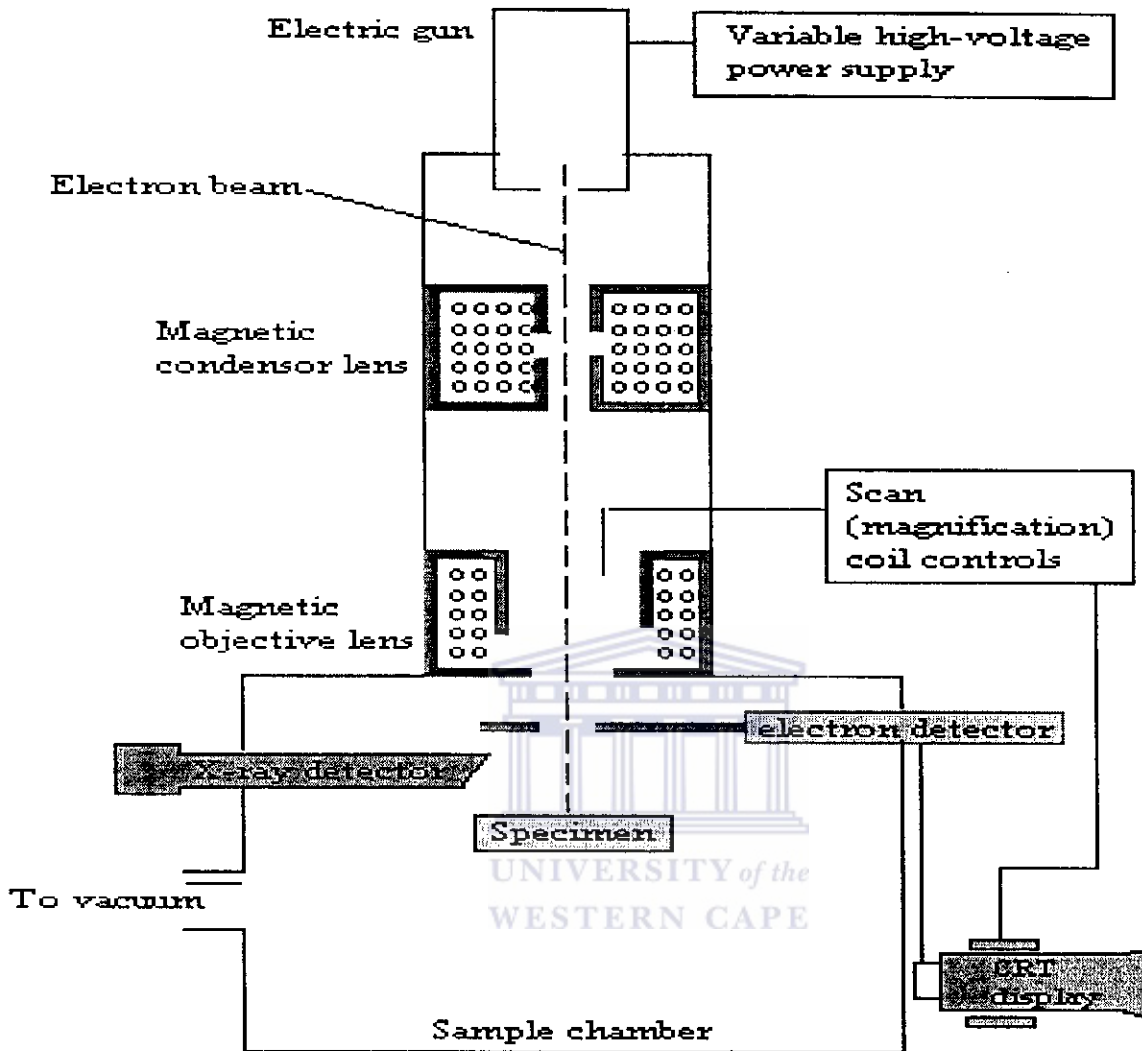


Figure 13: Schematic diagram of a SEM.

In Figure 13 is a schematic of a combined instrument that is both a scanning electron microscope and a scanning electron microprobe.

The SEM is primarily used to study the surface, or near surface structure of bulk specimens. An electron gun, usually of the tungsten filament thermionic emission type produces electrons, and accelerates them to energy between about 2keV and 40keV. Two or three condenser lenses then demagnify the electron beam until, as it hits the specimen, it may have a diameter of only 2-10nm.

The fine beam of electron is scanned across the specimen by the scan coils, while a detector counts the number of low energy secondary electrons, or other radiation, given off from each point on the surface. At the same time, the spot of a cathode ray tube (CRT) is scanned across the screen, while the amplified current from the detector modulates the brightness of the spot.

Methods and Instrument used

The following procedure was used for the characterisation of the catalysts and the titanium peroxide compounds before and after irradiation. The sample was placed on a stub after which it was coated with gold, Au, using the EDWARDS S150B sputter coater. Each stub was placed separately into the sample holder of the scanning electron microscope (HITACHI X650). Photographs were taken for morphology analysis.

3.3.4 Ultraviolet - Visible Spectroscopy (Vis/UV) ^{61, 63}

Ultraviolet visible spectroscopy is employed primarily for quantitative analysis and is probably more widely in chemical and clinical laboratories throughout the world than any other single procedure.

Ultraviolet spectrophotometric methods have been applied rather extensively to the identification of aromatic hydrocarbons, vitamins, steroids, heterocyclics, and conjugated aliphatic. In biochemical and pharmaceutical research, ultraviolet absorption spectra are often used to identify degradation products and to test for purity. The detection of characteristic ultraviolet absorption bands of contaminants is used as a guide to purity while the constancy of molar absorptivity at a specific wavelength upon additional purification steps is indicative of purity.

Ultraviolet absorption spectra are attributed to a process in which the outer electrons of atoms, or molecules, absorb radiant energy and undergo transitions to higher energy levels. These electronic transitions are quantized and depend on the electronic structure of the absorber. The magnitude of these discrete energy changes increases as the spectral position of the corresponding absorbance maximum goes from the visible to the shorter wavelength region. Thus, whereas perhaps 50,000 calories per mole may be involved for an absorption band in the visible region, 100,000 calories per mole are required for an absorption band in the ultraviolet region.

The wavelength at which an ultraviolet absorbance maximum is found depends on the magnitude of the energy involved for a specific electronic transition. The molar absorptivity depends on the rate at which the absorber is absorbing radiant energy from the incident beam. When the absorber is in the gaseous state, the vibrational and rotational transitions may also contribute to the characteristic absorption spectrum. The fine vibrational structure characteristic of a vapor usually disappears when the substance is dissolved in a solvent due to perturbation by the solvent molecules. The effect of the solvent on ultraviolet absorption spectra of certain solutes is often quite pronounced.

In the case of inorganic ions and molecules, the transitions may be between two electronic states of the individual atoms, or there may be a partial electron transfer from ligand to the central ion resulting in a charge - transfer absorption spectrum. It is possible for both the electronic transitions and the electron transfer process to contribute to the absorption spectrum of a substance.

Several types of transitions involving both bonding and nonbonding electrons are possible with organic substances. The transitions of electrons, which form single bonds (σ -electrons) from one orbital to a higher energy orbital, give absorption bands in the far ultraviolet.

Methods and instrument used

The GBC 920 Ultraviolet visible spectrophotometer was used. The sample was ground and placed into the solid sample holder for obtaining the reflectance spectrum.

3.4 IRRADIATION EXPERIMENTS

3.4.1 Schematic diagram of experimental apparatus

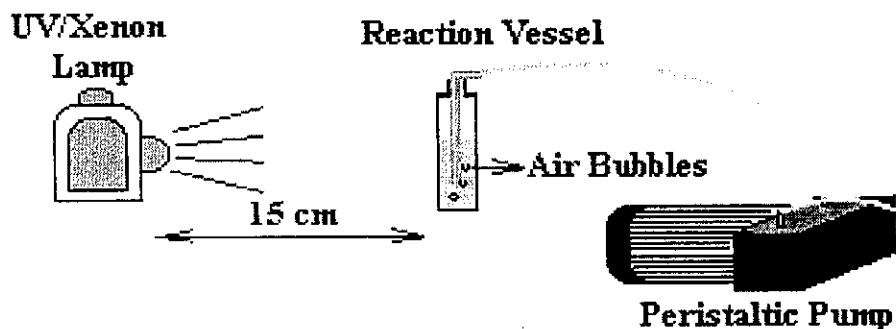


Figure 14: Experimental set-up

3.4.1.1 Reaction vessels

The reaction vessels are made of silica. Therefore the vessels are transparent to UV.

3.4.1.2 Xenon lamp

The electromagnetic radiation produced has a maximum peak intensity occurring at ~500nm. The lamp used was a 900W Xenon lamp.

3.4.1.3 UV lamp

The UV lamp used consists of a Phillips HPA metal halide with iron and cobalt additives. It has maximum emission intensity between 300 and 400nm.

3.4.2 Irradiation procedure

All catalyst systems used were placed in the reaction vessel and irradiated with either the Xenon lamp or UV lamp, respectively. The reaction vessel was placed at a distance of 15cm from the lamp. These samples were then irradiated for a measured time period under a flow of air at 1500ml/min. The irradiated samples were tested qualitatively (Diphenylamine reagent, etc.) and quantitatively (Merck Reflectoquant test strip analyser) for the presence of nitrite, NO_2^- and nitrate, NO_3^- . Section 3.5 consists of a detail description of these tests.

3.5 NITRATE, NO_3^- AND NITRITE, NO_2^- ANALYSIS

3.5.1 Qualitative Analysis

3.5.1.1 Test for NO_3^-

A. Diphenylamine reagent ⁶⁴

i. *Preparation*

The reagent was prepared by dissolving 0.5g diphenylamine in 85ml concentrated H_2SO_4 diluted to 100ml with water.

ii. *Procedure*

The nitrate sample was carefully poured down the side of the test tube so that it formed a layer above the diphenylamine reagent. A blue ring was formed between the two layers; indicating a positive test.



B: Brown ring test⁶⁴

Concentrated H_2SO_4 (4ml) was slowly added to the sample solution (2ml). Saturated FeSO_4 was slowly poured down the side of the tube so that it formed a layer above the H_2SO_4 layer. A brown ring was formed between the two layers, indicating a positive test.

3.5.1.2 Test for NO_2^-

Reduction of NO_3^- to NO_2^- ⁶⁴

The NO_3^- sample was reduced by the addition of Zn and HCl. This sample was then tested for the presence of NO_2^- , by addition of sulphanilic acid reagent followed by α -naphthylamine reagent, a red coloration indicating a positive test.

3.5.2 Quantitative Analysis



Merck Reflectoquant Test Strip Analyser

Besides the mobility enabled by this system, the innovative mini laboratory for on-the-spot analysis is characterized by its high measurement precision, its environmental compatibility, and its convincing price-performance ratio. The successful combination of high-combination of high-quality analytical test strips and specially developed, state-of-the-art evaluation technology has now made it possible to quantitatively assess the hitherto only qualitatively valuable test strips.

Bischoff ⁶⁵ et al investigated the comparisons of using test strips and two analytical laboratory methods for the analysis of nitrate. They found that a cost-effective alternative to laboratory analysis is dip-style test strips. Use of the strips, especially by non-technical persons, such as homeowners, provides a means to check for nitrate contamination without the expense involved in a detailed laboratory analysis. Several readers their results were then compared with the two analytical technique i.e. high performance liquid chromatography (HPLC) and colorimetric analysis using colorimetric ion analyser did the dip-style experiment test.

Table 3: Analysis of nitrate concentration (ppm) by nitrate test strips and two other analytical methods.

Sample Std	Reader 1	Reader 2	Reader 3	Ion Analysis	HPLC
1	1	1	1	1.22	BLD
5	5	5	2	4.98	5.10
10	10	10	5	9.97	10.31
50	50	50	50	49.2	50.74

The results obtained are remarkably similar between the readers and the two techniques. Evaluation of nitrate test strips used in the field indicates that they can be a reliable quick test nitrate contamination. The use of test strips for screening purposes to evaluate potential wells for further study in a research project would also save time and expense. The colorimetric and HPLC nitrate analysis data agree very closely with the test strip analysis results.

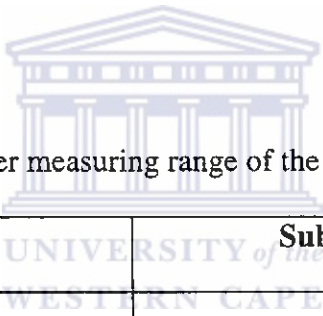
3.5.2.1 Nitrite Test Strip Analyser

Application

The nitrite test strips was used to determine the nitrite ion (NO_2^-) in the liquid samples before and after irradiation. This nitrite test strips analyser was used because of the low concentration detection limit and the quick reaction time of 15 seconds. The measuring range we used was between 0.5-25.0mg/l for the detection of nitrite ion (NO_2^-).

Table 4 below shows the measuring ranges of nitrogen and nitrite ion detected using the nitrite test strips.

Table 4: The RQflex reflectometer measuring range of the nitrite test strips.



Measuring range	Substance
0.5 - 25.0 mg/l	NO_2^-
0.2 - 7.6 mg/l	N
10.9 - 542 mmol/m ³	N or NO_2^-

Method

In the presence of an acidic buffer, nitrite reacts with an aromatic amine to form a diazonium salt, which in turn reacts with N-(1-naphthyl)-ethylenediamine to form a red-violet azo dye, the concentration of which is determined reflectometrically.

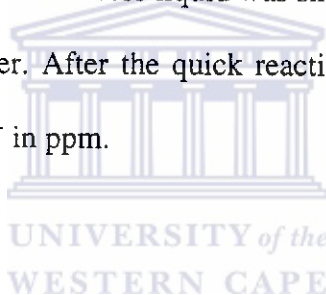
Preparation of the sample

If the pH of the samples was not between 1-13, and the pH was lower than 1, it was buffered with sodium acetate; if greater than 13, it was adjusted to approximately 3 to 5 with tartaric acid.

The suspended catalyst was filtered off after irradiation and the filtrate analysed for nitrite.

Procedure for the nitrite test

The nitrite test strip was immersed in to the sample solution for 2 seconds. The strip was removed from the sample and the excess liquid was shaken off. The test strip was then inserted into the strip adapter. After the quick reaction time of 15 seconds the result displayed is that of the NO_2^- in ppm.



Note:

1. If the test strip was inserted into the adapter after the reaction time had expired, the test strip was discarded because it resulted in a false-high reading of the nitrite concentration.
2. Samples containing more than 25mg/l NO_2^- were diluted with distilled water.

3.5.2.2 Nitrate Test Strip Analyser

Application

The nitrate test strips was used to determine the nitrate ion (NO_3^-) in the liquid samples before and after irradiation. This nitrate test strips analyser was used because of the low concentration detection limit and the quick reaction time of 60 seconds. The measuring ranges for the nitrate test strip are shown in table 5 below.

Table 5: The RQflex reflectometer measuring range of the nitrate test strips.

Measuring range	Substance
3 - 90 mg/l	NO_3^-
0.7 - 20.3 mg/l	N
48.3 - 1449 mmol/m ³	N or NO_3^-

The measuring range used in the analysis for the presence of nitrate ion (NO_3^-) was between 3-90mg/l.

Method

A reducing agent reduces nitrate to nitrite. In the presence of an acidic buffer, this nitrite reacts with an aromatic amine to form a diazonium salt, which in turn reacts with N- (1-naphthyl)- ethylenediamine to form a red-violet azo dye, the concentration of which is determined reflectometrically.

Preparation of samples

If the pH of the samples was not between 1-12, and the pH was lower than 1, it was buffered with sodium acetate; if greater than 12, it was adjusted to approximately 3 to 5 with tartaric acid.

The suspended catalyst was filtered off after irradiation and the filtrate analysed for nitrate. The nitrite content was checked in the sample. Adding 5 drops of a 10% aqueous amidosulfonic acid solution to 5ml of the sample with pH less than 10 eliminated interfering nitrite ions. The sample was shaken several times and the nitrate and nitrite ion content checked.

Procedure for the nitrate test

The nitrate test strip was immersed in to the sample solution for 2 seconds. The strip was removed from the sample, excess liquid was shaken off and inserted into the strip adapter. After the quick reaction time of 60 seconds the result displayed is that of the NO_3^- in ppm.

Note:

1. If the test strip was inserted into the adapter after the reaction time has expired, the test strip was discarded because it resulted in a false-high reading of the nitrate concentration.
2. Samples containing more than 90mg/l NO_3^- were diluted with distilled water.

Chapter 4

RESULTS *and* DISCUSSION

of

CATALYSTS CHARACTERISATION

UNIVERSITY *of the*
WESTERN CAPE

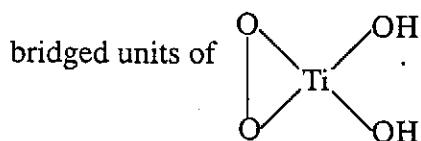
4.1 FTIR STUDIES ON PEROXO TITANIUM COMPOUNDS

4.1.1 Introduction

The titanium peroxide compounds were prepared in two different ways by using Method I (see 3.2.1) and Method II (see 3.2.1).

The peroxytitanium (IV) compounds have been intensively studied by many researchers.^{56, 57} Researchers such as Piccini⁶⁶ and Weller⁶⁷ prepared "titanium peroxide", but the composition of their products differed. The molar ratio of $\text{TiO}_2:\text{O}_{\text{peroxy}}$ for the peroxide synthesized by Piccini⁶⁶ is 1:0.5 while that by Weller⁶⁷ is 1: 0.61-0.81.

Peroxide studies by Levy⁶⁸ suggested the following three alternative formulae: TiO_3 ; $\text{TiO}_2 \cdot \text{H}_2\text{O}_2$ or $\text{Ti}_2\text{O}_5 \cdot \text{H}_2\text{O}_2$. Whereby Mc Kinney⁶⁹ et al suggested that for Ti_2O_5 the peroxide structure was a five membered ring. Kharkar⁷⁰ et al found that the freshly prepared peroxide corresponded to $\text{TiO}_3 \cdot x\text{H}_2\text{O}$ and represented the peroxide as



They found that the peroxide lost its peroxy oxygen content and after eight days it transformed to Ti_2O_5 , being a mixture of TiO_3 and its degradation product, TiO_2 . Jere⁵⁷ et al determined that the peroxide has an unstable peroxy group and two hydroxyl groups for every titanium atom. The compound produced was identified as peroxide and not a perhydrate by using the Reisenfeld-Liebhofsky test⁷¹.

Jere⁵⁷ et al has reported the infrared spectra of a number of hydrated polymeric peroxy-titanium complexes. The two bands close to 1053cm^{-1} were assigned to the antisymmetrical stretching mode of vibration of Ti-O, while that at 885cm^{-1} to the symmetrical stretching mode of vibration of the Ti-O ring structure. The hydrogen bonded hydroxyl group has a broad band in the region of about 3175cm^{-1} and a medium intensity band in a region of 1681cm^{-1} .

4.1.2 Results

When comparing the FTIR spectra obtained with that of the literature it could be concluded that a titanium peroxide compound was formed. Figure 15 shows the FTIR spectra of the titanium peroxide compound obtained. The broad band in the region of $\sim 3384.3\text{cm}^{-1}$ and a medium band at 1646cm^{-1} according literature was identified as due to $\nu(\text{O-H})$ stretching vibration in hydroxyl groups. The peaks at 1120cm^{-1} and 872cm^{-1} are due to $\nu(\text{Ti-O})$ stretching vibrations according to literature.

The peak at 1120cm^{-1} according to the literature may be a sulphate group because of the oxotitanium (IV) sulphate used as starting material. Due to this problem method II was adopted where the titanium hydroxide was used as starting material. The product we obtained was in a gel form, therefore no FTIR spectra were obtained for these compounds.

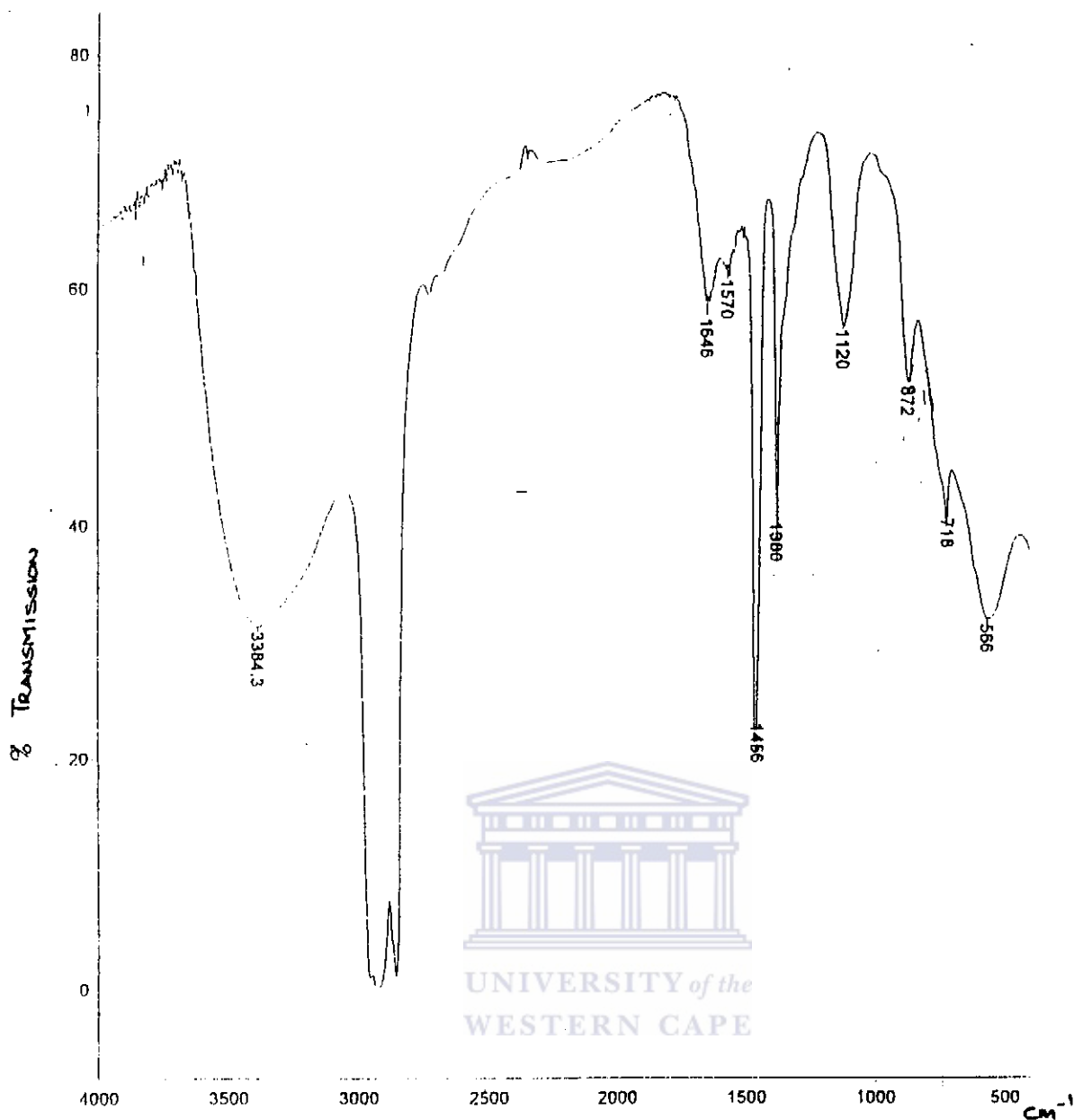


Figure 15: FTIR spectra of the titanium peroxide compound prepared by Method I.

4.2 BANDGAP ENERGIES USING THE VIS/UV SPECTROSCOPY

Visible absorption spectroscopy can be used to measure the bandgap energy, that is, the energy gap between the lower energy filled band, known as the valence band, and the higher energy empty band, known as the conduction band. Solids with bandgap energies less than 3eV are considered to be semiconductors while insulators have bandgap energies larger than 3eV.

Titanium Peroxide Compounds: Absorbance versus Wavelength (nm)

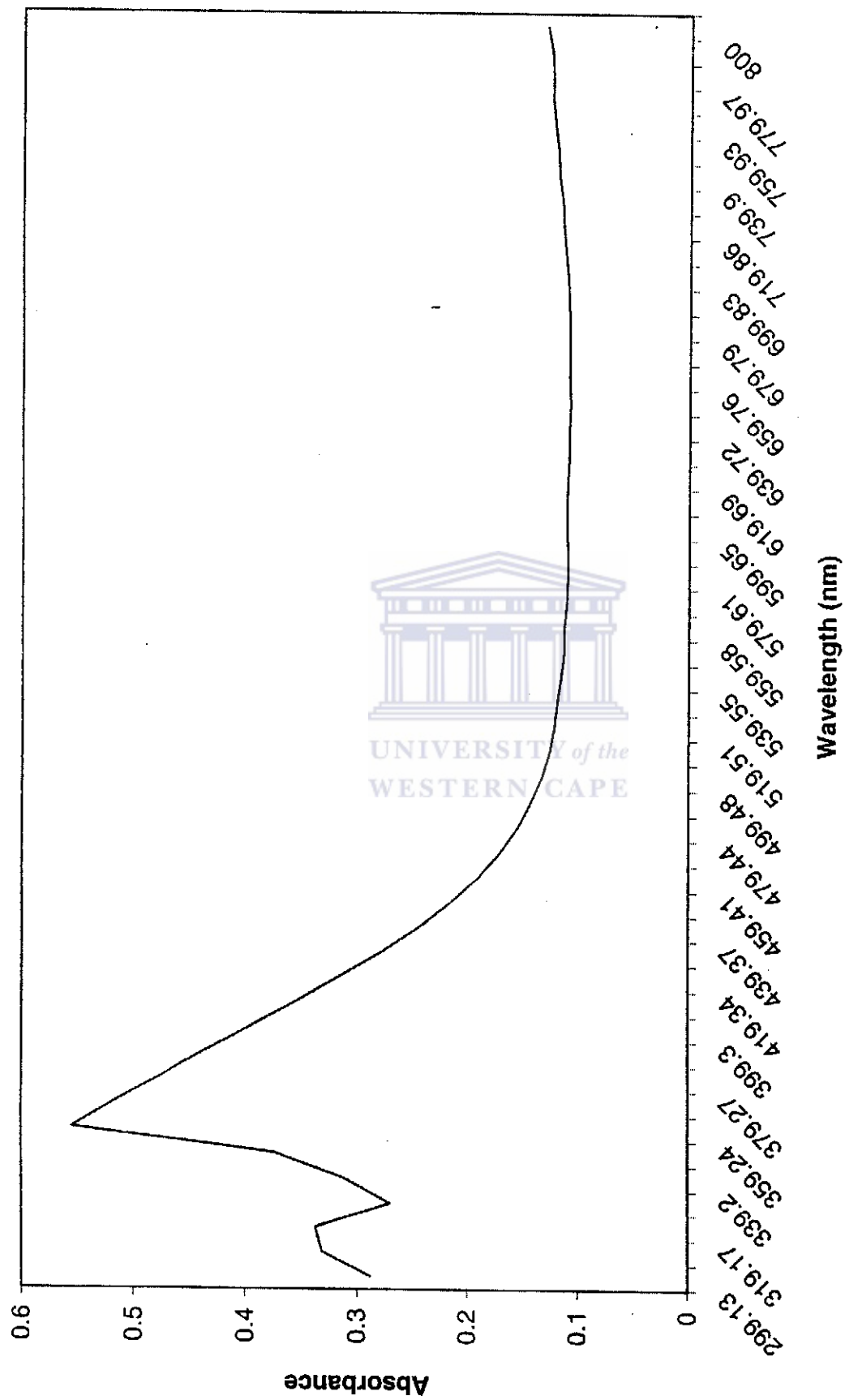


Figure 16: The Vis/UV spectra of titanium peroxide compound prepared by Method I.

Titanium dioxide (Degussa P25): Absorbance versus Wavelength

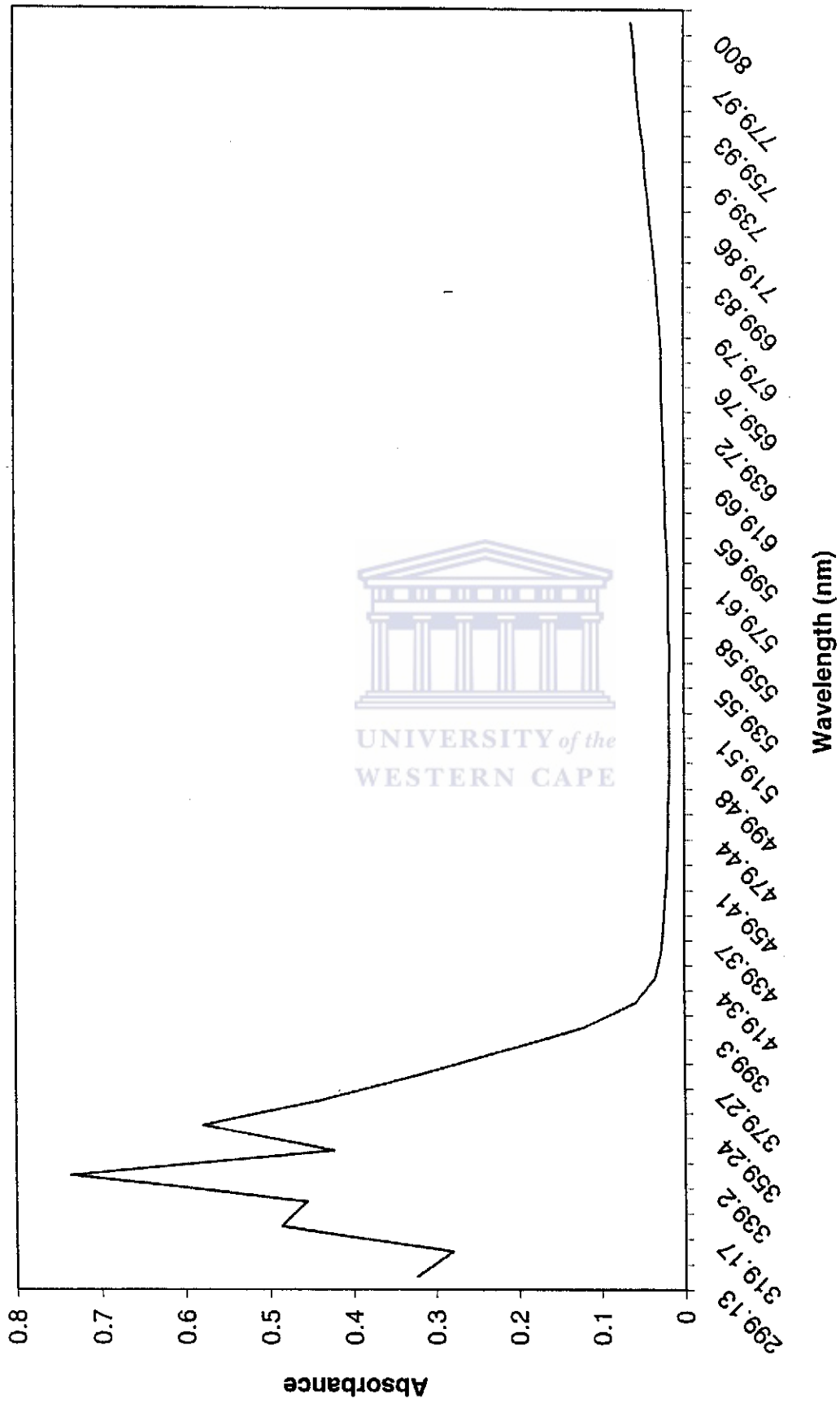


Figure 17: The Vis/UV spectrum of the Degussa P25.

Titanium dioxide (rutile): Absorbance versus Wavelength (nm)

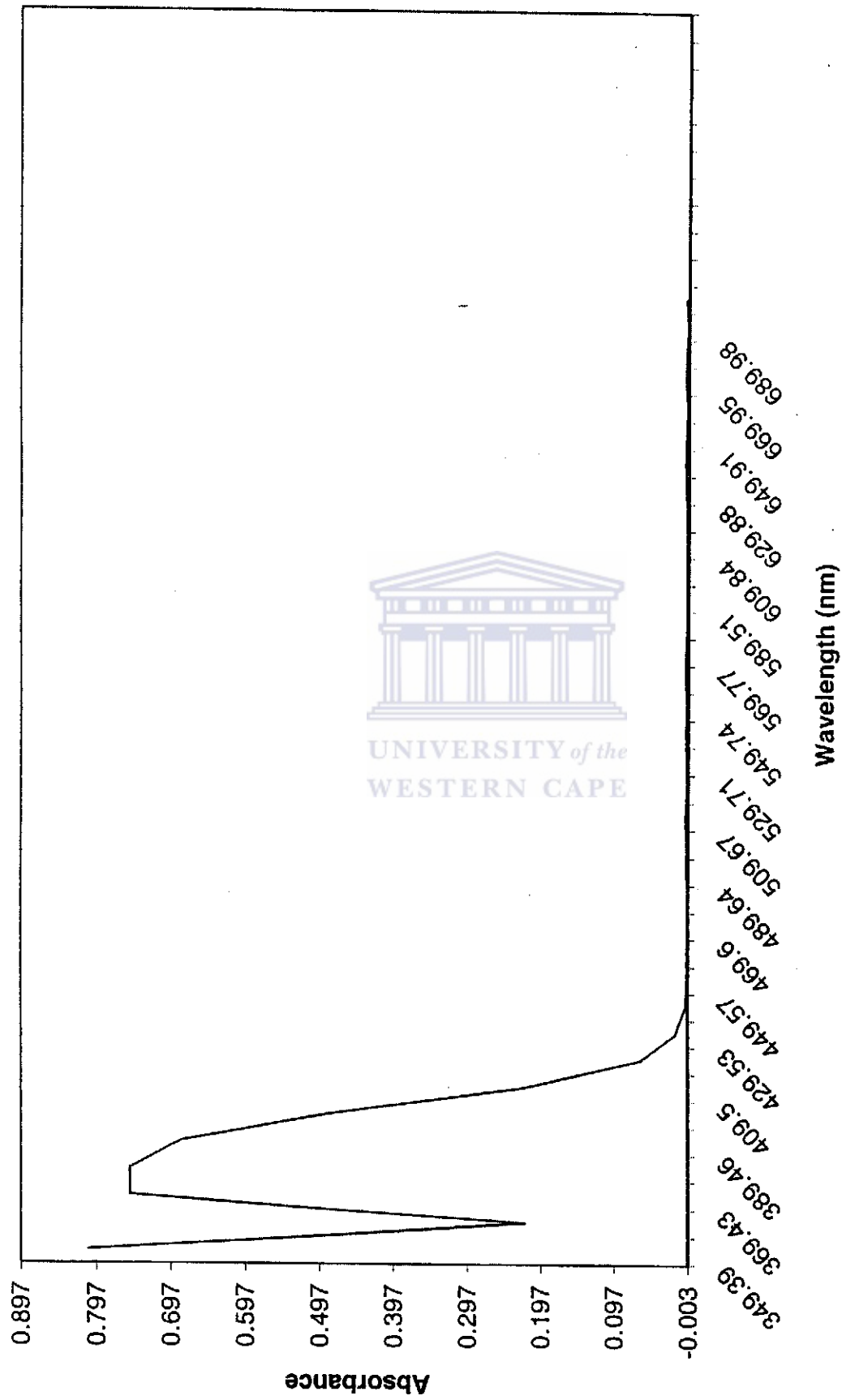
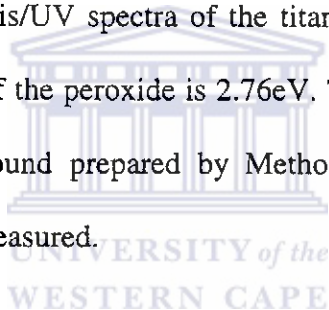


Figure 18: The Vis/UV spectrum of TiO₂(rutile).

Table 6: The bandgap energies and wavelengths of some possible catalysts obtained from the Vis/UV spectra.

Catalyst	Wavelength (nm)	Band gap energies, E_{bg} (eV)
TiO ₂ (Degussa P25)	410	3.03
TiO ₂ (rutile)	390	3.18
Titanium peroxide	450	2.76

In Figure 16 above, show the Vis/UV spectra of the titanium peroxide prepared by Method I. The bandgap energy of the peroxide is 2.76eV. Thus the titanium peroxide is a semiconductor. The compound prepared by Method II was a gel hence the Vis/UV spectrum could not be measured.



The bandgap energies of Degussa P25 (i.e. mixture of anatase and rutile) and rutile were also obtained. The Vis/UV spectra are shown in Figure 17 and 18, respectively. The bandgap energy of rutile is measured at 3.03eV and corresponds to a photon of 410nm and of Degussa P25 is 3.18eV and corresponds to a photon of 390nm. The results obtained correspond to those in the literature.

4.3 MORPHOLOGY ANALYSIS OF THE CATALYSTS

The morphology of these compounds was studied using the scanning electron microscopy (SEM). The SEM provides morphology and topographic information about the surfaces of solids that is usually necessary in understanding the behaviour of surfaces.

The titanium peroxide compound prepared by Method II was a gel hence the morphology could not be analysed. The compound by method I was discarded because of the possible contamination of the sulphate group.

The Degussa P25, RBM concentrated rutile and RBM rutile flour of the surface area was analysed. In Figure 19, 20 and 21 shows the SEM morphology of the Degussa P25, RBM concentrated rutile and rutile flour, respectively.

In Figure 19, that is the electron micrograph of the Degussa P25 with the magnification at 1.01K show that the samples are fine particles and which are clustered together. In the micrograph of the Degussa P25 the surface is observed to be rough.

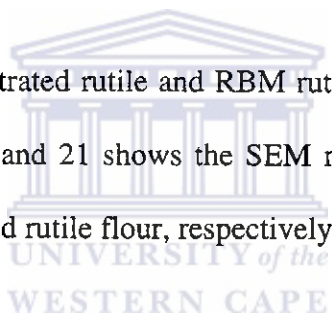
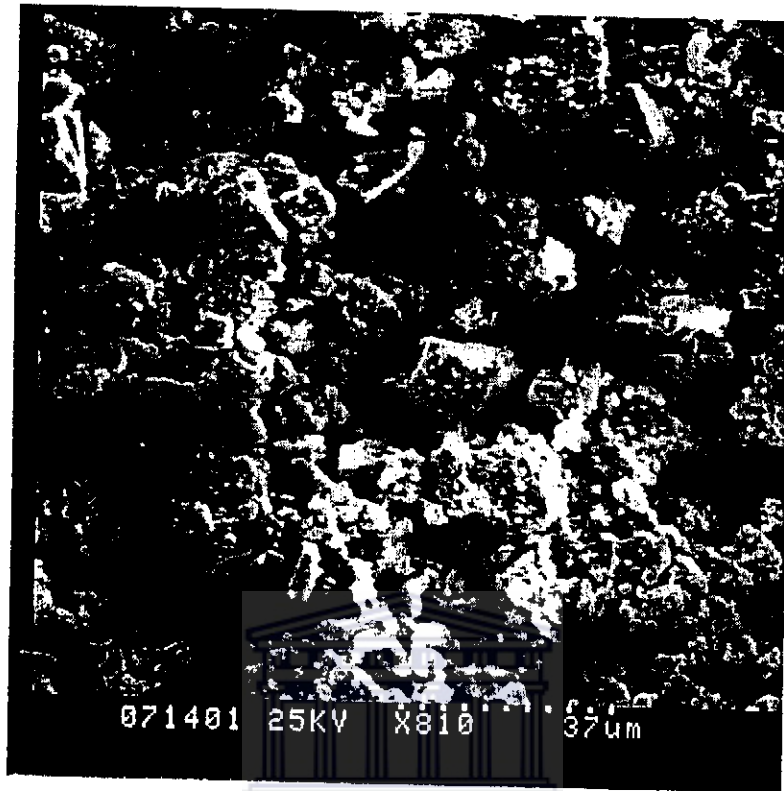




Figure 19: Electron micrograph of Degussa P25.

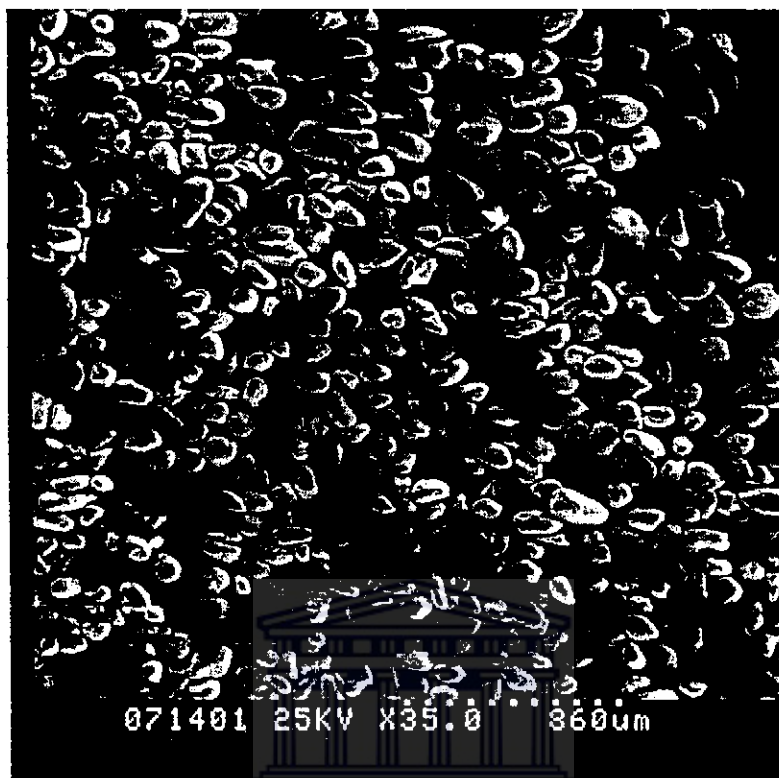
In Figure 20, the electron micrograph of the RBM rutile flour is shown, the micrograph was taken at magnification at 810. The surface of this sample was observed to be rough. The particles are not compact like that of the Degussa P25. The micrograph obtained shows that the particle sizes of the RBM rutile flour although small are not smaller than those of Degussa P25 (see Figure 19).



UNIVERSITY of the
WESTERN CAPE

Figure 20: Electron micrograph of RBM rutile flour.

In Figure 21 below show the electron micrograph of the RBM concentrated rutile with its at magnification at 35. The micrograph shown in Figure 21 show that the RBM concentrated rutile is single multi-shape beads, which is loosely arranged. The surface of this sample was observed to be very smooth.



UNIVERSITY of the
WESTERN CAPE

Figure 21: Electron micrograph of RBM concentrated rutile.

From this information we can conclude that the surface area of these catalysts are in the following order: RBM concentrated rutile < RBM rutile flour < Degussa P25. Since particle sizes are in the order RBM concentrated rutile >RBM rutile flour > Degussa P25.

Chapter 5

RESULTS *and* DISCUSSION

of

IRRADIATION EXPERIMENTS

UNIVERSITY *of the*
WESTERN CAPE

5.1 EFFECT of using DIFFERENT SOLID COMPOUNDS as CATALYSTS

Blank experiments (see section 5.2) are a necessity to be carried out in order to find out if the reactions require: a solid photocatalyst (see section 5.2.1), air (see section 5.2.2) and irradiation (see section 5.2.3) for producing NO_3^- and/or NO_2^- .

5.1.1 Comparison of the different forms of titanium peroxide

Using compounds prepared by method I and II (see section 3.2.1), each of these compounds was suspended in a pH 14 solution and irradiated using a Xenon lamp. Table 7 below shows the data obtained.

Table 7: Concentration of NO_3^- and NO_2^- obtained using titanium peroxide compounds (conditions described in section 3.2.1) as the photocatalyst. Irradiation was carried out using the Xenon lamp passing air through a 90ml sample at 1500ml/min.

Description	Method I		Method II	
	NO_2^- (ppm)	NO_3^- (ppm)	NO_2^- (ppm)	NO_3^- (ppm)
1. Before irradiation.	LO	LO	LO	LO
2. Irradiated for 2hrs.	LO	LO	LO	3
3. Irradiated for another 4hrs.	LO	LO	LO	5

*Note: Below detection limit range (LO).

NO_3^- was detected using the titanium peroxide from Method II. As the irradiation time increased the NO_3^- concentration increased slightly. Neither NO_3^- nor NO_2^- could be detected using titanium peroxide from Method I.

5.1.2 Degussa P25 TiO_2

Degussa P25 treated with H_2O_2 was prepared (see section 3.2.2) and used as the photocatalyst. Table 8 below shows the concentration of NO_3^- and NO_2^- obtained using the following conditions 0.5g of Degussa P25 treated with 20ml of 20% H_2O_2 at pH 14.

Table 8: Concentration of NO_3^- and NO_2^- obtained using Degussa P25 (conditions described in section 3.2.2) as the photocatalyst. Irradiation was carried out using the Xenon lamp passing air through a 90ml sample at 1500ml/min.

Description	NO_2^- (ppm)	NO_3^- (ppm)
1. Before irradiation.	LO	LO
2. Air was passed through sample and irradiated for 2hrs.	LO	5
3. Irradiated for a further 4hrs.	LO	17

*Note: Below detection limit range (LO).

NO_3^- was detected after irradiation. The concentration of the NO_3^- species increased with increasing time of irradiation.

5.1.3 Comparing the effect of the uses of different photocatalysts

The results from 5.1.1 and 5.1.2 are summarised in Figure 22. The next step was then to find the most effective solid photocatalyst for the production of nitrate.

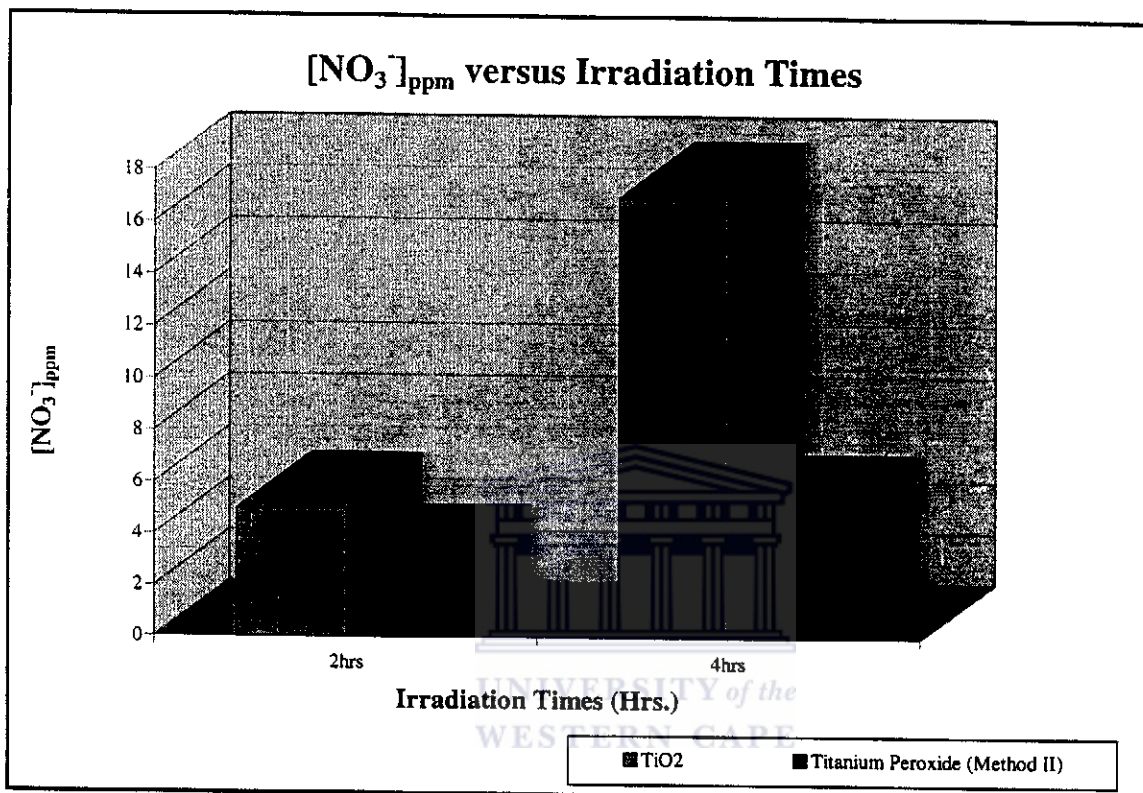


Figure 22: Comparison of the Degussa P25 and titanium peroxide used as photocatalysts.

The Degussa P25 photocatalyst takes only 2hrs to prepare compared to the preparation of titanium peroxide in Method II that takes more than 2 days to be prepared. The resulting nitrate concentration obtained, using Method II samples (that is, titanium peroxide) as photocatalysts (prepared in section 3.2.1) was compared with the resulting nitrate concentration obtained using Degussa P25 samples as photocatalysts.

From Figure 22, it can be seen that as the irradiation times increased the concentration of NO_3^- increased. After 2hrs of irradiation the concentration of NO_3^- produced using Degussa P25 was greater than that when using titanium peroxide. When the samples were irradiated for further periods the same trend continued.

So not only are the Degussa P25 photocatalysts easier and quicker to prepare they produce more NO_3^- than those of titanium peroxide. Thus Degussa P25 was chosen as the photocatalyst for testing other experimental variables.

5.2 BLANK EXPERIMENTS

The following were investigated:

- the requirement of a solid photocatalyst
- the requirement of air (i.e. O_2 and N_2)
- the requirement of irradiation.

The approach that has been taken was to run several blank experiments not only to find out if a solid catalyst is needed for the reaction but also to find out if irradiation, the passing of air through the sample and H_2O_2 are also required.

5.2.1 Requirement of a solid photocatalyst

Table 9 below shows the concentration results of NO_3^- and NO_2^- obtained where no catalyst was present in the reaction mixture with 20ml of 20% H_2O_2 at pH 14.

Table 9: Concentration of NO_3^- and NO_2^- obtained where no catalyst was used at pH 14. Irradiation was carried out using a Xenon lamp.

Description	Hrs	$[\text{NO}_3^-]$ (ppm)	$[\text{NO}_2^-]$ (ppm)
1. Before irradiation		LO	LO
2. Ar was passed through the sample before irradiation.	1	LO	LO
3. Air was passed through the sample before irradiation.	1	LO	LO
4. Air gas was passed through the sample with irradiation.	4	LO	LO

*Note: The flow rate of the gas is 1500ml/min through a 90ml sample.

UNIVERSITY of the
WESTERN CAPE

No detectable NO_3^- or NO_2^- was produced in the absence of a solid catalyst under the above conditions.

5.2.2 Requirement of air

Argon, Ar gas was used in place of air in the presence of a Degussa P25 solid TiO_2 photocatalyst. Table 10 below shows the concentration of NO_3^- and NO_2^- obtained using the following conditions 0.5g of Degussa P25 treated with 20ml of 20% H_2O_2 at pH 14.

Table 10: Concentration of NO_3^- and NO_2^- obtained using the Degussa P25 (conditions described in section 3.2.2) as a photocatalyst irradiated with the Xenon lamp.

Description	Hrs	$[\text{NO}_3^-]$ (ppm)	$[\text{NO}_2^-]$ (ppm)
1. Before irradiation		LO	LO
2. Ar gas was passed through the sample without irradiation.	2	LO	LO
3. Ar gas was passed through the sample with irradiation.	4	1	LO
4. Ar gas was passed through the sample with irradiation.	6	1	LO

*Note: The flow rate of the gas is 1500ml/min through a 90ml sample.

Very little NO_3^- was detected using argon gas in place of air. The reason for detecting a small concentration of NO_3^- might be that the reaction vessel was not properly sealed therefore the sample was not properly degassed.

5.2.3 Requirement of irradiation

Table 11 below shows the concentration of NO_3^- and NO_2^- obtained using the following conditions 0.5g of Degussa P25 treated with 20ml of 20% H_2O_2 at pH 10.

Table 11: NO_3^- and NO_2^- concentration obtained using Degussa P25 (conditions described in section 3.2.2). Irradiation was carried out the using the Xenon lamp passing air through a 90ml sample at 1500ml/min.

Description	$[\text{NO}_3^-]$ (ppm)	$[\text{NO}_2^-]$ (ppm)
1. Before irradiation.	LO	LO
2. Ar was passed through the sample for 2hrs without irradiation.	LO	LO
3. For another 4hrs Ar was passed without irradiation.	LO	LO
4. Air was passed through the sample for 1hr without irradiation.	2	LO
5. Irradiation was continued for 1hr.	16	LO
6. Irradiation was continued for another 2hrs passing Air.	21	LO
7. Continued irradiation for another 4hrs passing Air.	22	LO

Although some NO_3^- was formed without irradiation the amount produced markedly increased upon use of Xenon lamp irradiation.

5.2.4 Effect of the Xenon or UV lamp irradiation

The results in table 12 were obtained using either the Xenon and UV lamp with the following experimental conditions 0.5g of Degussa P25 treated with 20ml of 20% H_2O_2 at pH 4. The sample was irradiated for 2hrs, followed by a further irradiation of 4hrs passing air at 1500ml/min through a 90ml sample.

Table 12: Concentration of NO_3^- and NO_2^- obtained with variation of the irradiation source (i.e. the Xenon and UV lamp).

Description	Xenon		UV	
	NO_2^- (ppm)	NO_3^- (ppm)	NO_2^- (ppm)	NO_3^- (ppm)
1. Before irradiation.	LO	LO	LO	LO
2. Irradiated for 2hrs.	LO	23	LO	26
3. Irradiated for further 4hrs.	LO	30	LO	33

The wavelength change from white light (Xenon) to low energy UV (UV lamp) does not have a great effect on the concentrations of NO_3^- produced.

From the results obtained, (see section 5.2) not only does the reaction require a solid photocatalyst (see section 5.2.1) but it also needs to be pretreated with H_2O_2 (see section 5.3.2) and air (see section 5.2.2) under irradiation (see section 5.2.3) for NO_3^- formation.

5.2.5 Summary

A solid photocatalyst of Degussa P25 in the presence of aqueous H_2O_2 and air under white light irradiation is required for NO_3^- formation under the described experimental conditions.

5.3 INVESTIGATION of FURTHER VARIABLES on OXIDATIVE NITROGEN FIXATION using Degussa P25 as PHOTOCATALYSTS.

The following variables were investigated using 90ml of reaction mixture and air:

- different pH values: 2, 4, 6, 8, 10, 12 and 14.
- different concentrations of H₂O₂: 0, 5, 10, 15, 20, 25 and 30%.
- different masses of the Degussa P25 photocatalyst: 0.1, 0.2, 0.3, 0.4, 0.5 and 1.0g.

5.3.1 Effect of different pH-values

The effect of different pH-values (i.e. = 2, 4, 6, 8, 10, 12 and 14) were investigated using Degussa P25 as the photocatalyst.

There are several reasons for this investigation:

- (i) the structure of titanium peroxide according to literature changes⁵⁶ at different pH values.
- (ii) the NO₃⁻ species is stable at lower pH values (i.e. in acidic region), where the NO₂⁻ species is more at higher pH values (i.e. in the basic region).
- (iii) the free energy change of the overall oxidation of N₂ is pH dependent.
- (iv) the bandgap energy of TiO₂ is also pH dependent.

Figure 23 below shows the concentration of NO_3^- obtained using the following experimental conditions 0.5g of Degussa P25 which was treated with 20ml of 20% H_2O_2 at different pH values. All these reactions were carried out individually at pH of 2, 4, 6, 8, 10, 12 and 14. The sample was irradiated using a Xenon lamp.

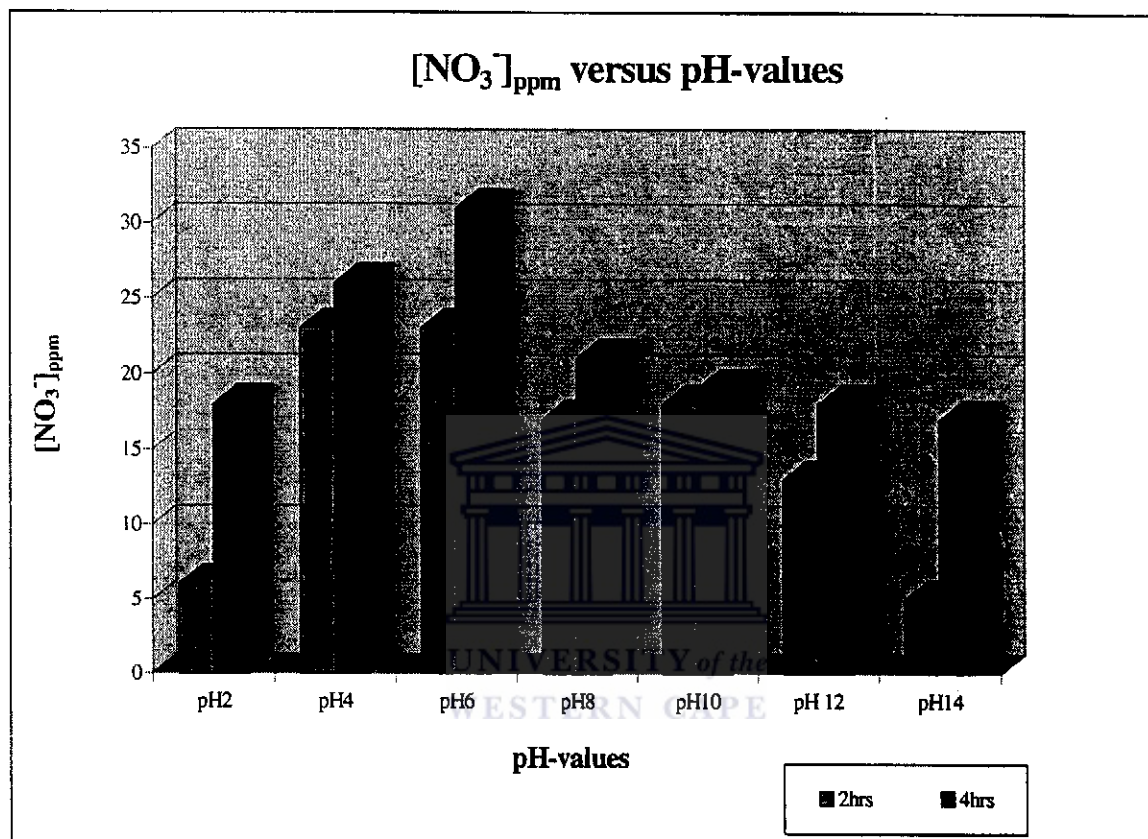


Figure 23: The effect of different pH-values using Degussa P25 as the photocatalyst. Irradiation was carried out using the Xenon lamp passing air through a 90ml sample at 1500ml/min.

The results obtained show that the pH has an influence on the concentration of nitrate produced. It can be seen that the concentration of NO_3^- produced is higher under acidic conditions than the basic conditions.

Figure 23 shows that the concentration of the NO_3^- increased as the irradiation time increased. The maximum concentration of NO_3^- was achieved at pH 4-6. No NO_2^- was detected presumably because under the highly oxidising conditions NO_3^- is the more stable species.

5.3.2 Effect of the concentration of H_2O_2

As mentioned before the N_2 does not chemisorb on TiO_2 but does when the TiO_2 is treated H_2O_2 . The effect of the concentrations of H_2O_2 was investigated to find the appropriate concentration of H_2O_2 , to produce the maximum concentration of NO_3^- . Thus Degussa P25 was treated with different concentrations of H_2O_2 of 5, 10, 15, 20, 25 and 30%.

Figure 24 below shows the effect the concentration of H_2O_2 has on the reaction using the following experimental conditions 0.5g of Degussa P25 treated with 20ml of different concentrations of H_2O_2 at pH 4. Irradiation was carried out using the Xenon lamp passing air at 1500ml/min through a 90ml sample.

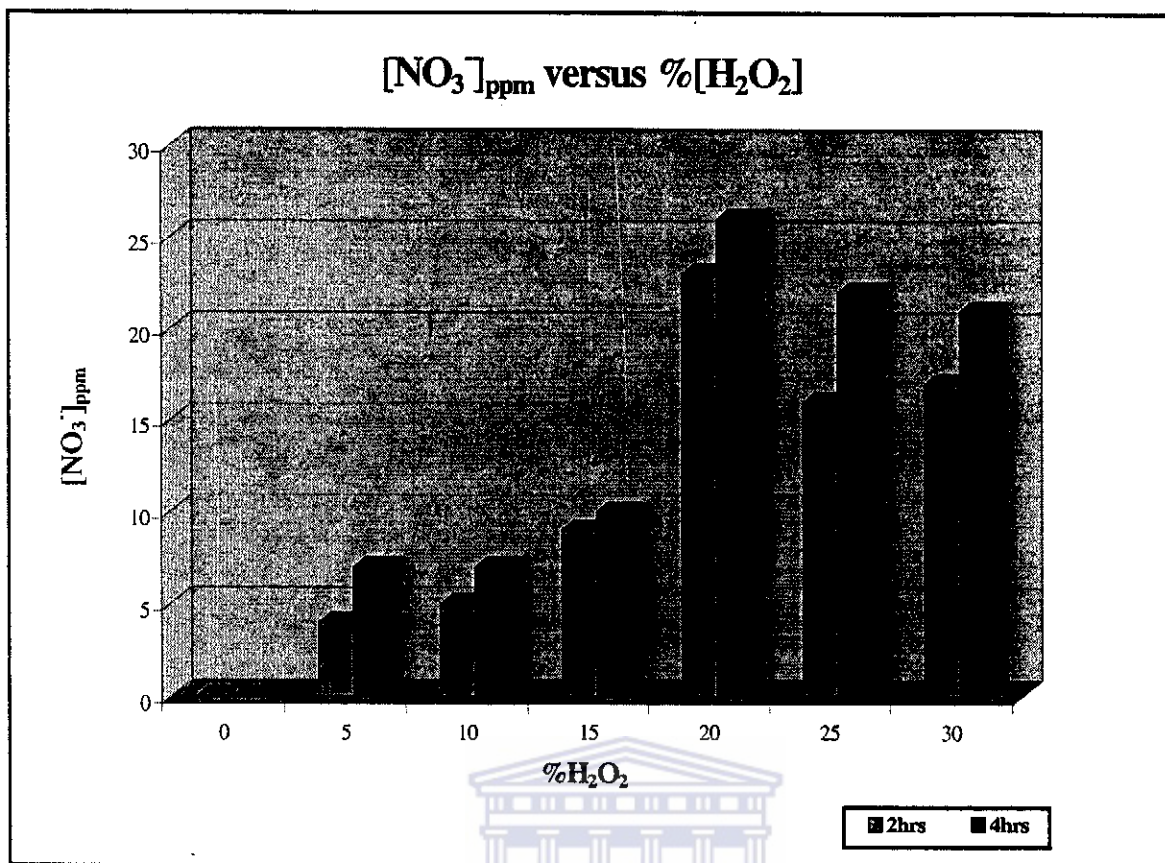


Figure 24: The effect of the concentration of H₂O₂ using Degussa P25 as the photocatalyst at pH 4. Irradiation was carried out using the Xenon lamp.

Figure 24 indicates the necessity of H₂O₂ as a reactant since NO₃⁻ was not formed in the absence of H₂O₂. The use of 20% H₂O₂ generated the highest NO₃⁻ concentrations. From the results obtained high H₂O₂ concentrations (i.e. 20%) produced two times the concentration of NO₃⁻ compared to that with lower H₂O₂ concentrations (i.e. 5%). The maximum concentration of NO₃⁻ was achieved at 20% H₂O₂. The H₂O₂ treatments cause the peroxide formation on the TiO₂ surface this in turn will alter with changing H₂O₂ concentration used. The degree and nature of the peroxidation will in turn affect the chemisorption of N₂ on that surface.

5.3.3 Effect of Mass of Catalyst

Figure 25 shows the influence the mass of the Degussa P25 on the formation of NO_3^- . The mass of the catalyst will affect the surface area available for the catalysis of the reactants to proceed.

The following experimental conditions were used for this investigation 0.1, 0.2, 0.3, 0.4, 0.5 and 1.0g of Degussa P25 were treated with 20ml of 20% H_2O_2 at pH 4. All these reactions had been carried out individually where the sample was irradiated using a Xenon lamp.

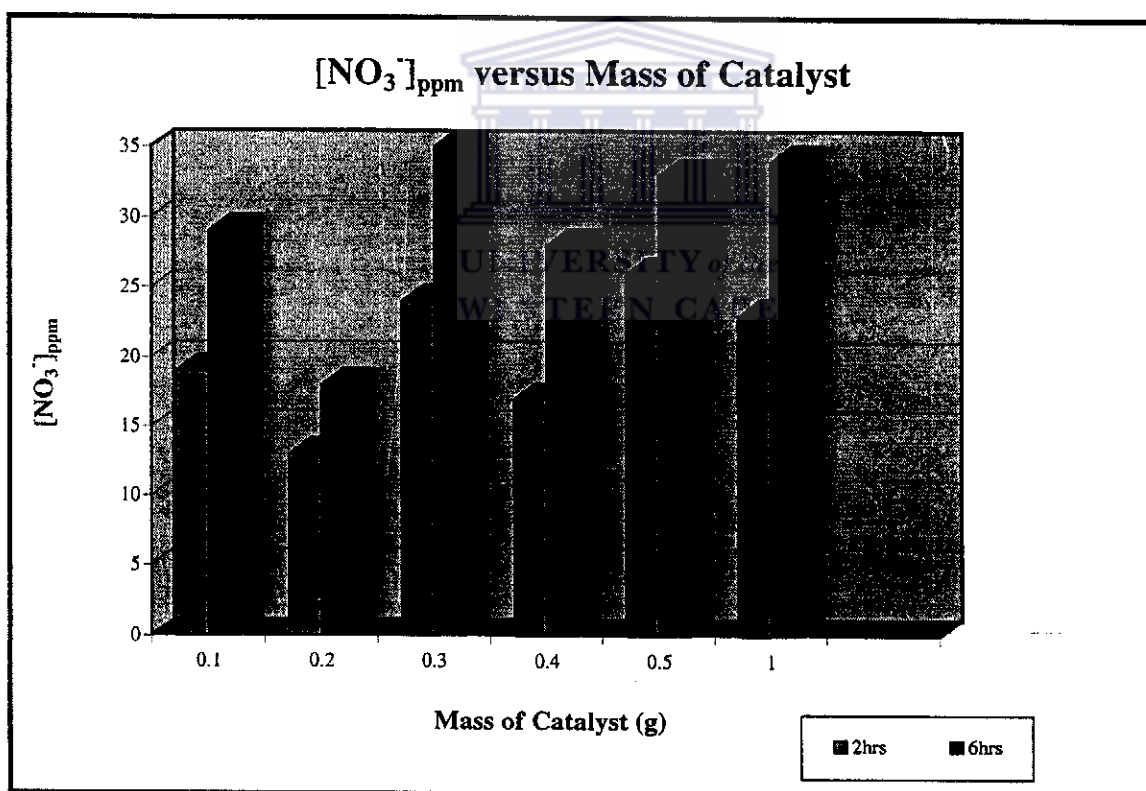
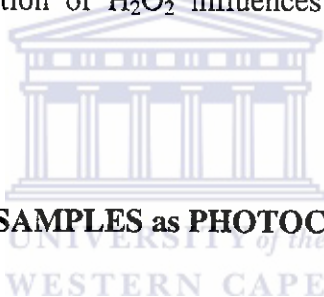


Figure 25: The effect of the mass of catalyst (Degussa P25) at pH 4 using the Xenon lamp for irradiation. Air was passed through a 90ml sample at 1500ml/min.

Once again in Figure 25 it can be seen that as the irradiation time increased the concentration of the NO_3^- also increased. Under the conditions used increasing the mass of catalyst above a certain value (0.1g) did not increase the concentration of NO_3^- obtained. However, this was obtained at a constant flow rate of reactant gases. Variation of flow rates must be included in future experiment.

5.3.4 Summary

The variables such as the pH-values, the concentration of H_2O_2 and the mass of the photocatalyst were intensively investigated. From the results it can be conclude that the pH used and the concentration of H_2O_2 influences the concentration of NO_3^- obtained.



5.4 USE of RBM RUTILE SAMPLES as PHOTOCATALYSTS

Samples used were:

1. RBM rutile flour
2. RBM concentrated rutile

Figure 26 below shows the concentration of NO_3^- obtained using the RBM rutile flour and RBM concentrated rutile as photocatalysts. The following conditions was used in both experiments 0.5g of photocatalyst treated with 20ml of 20% H_2O_2 at pH 4.

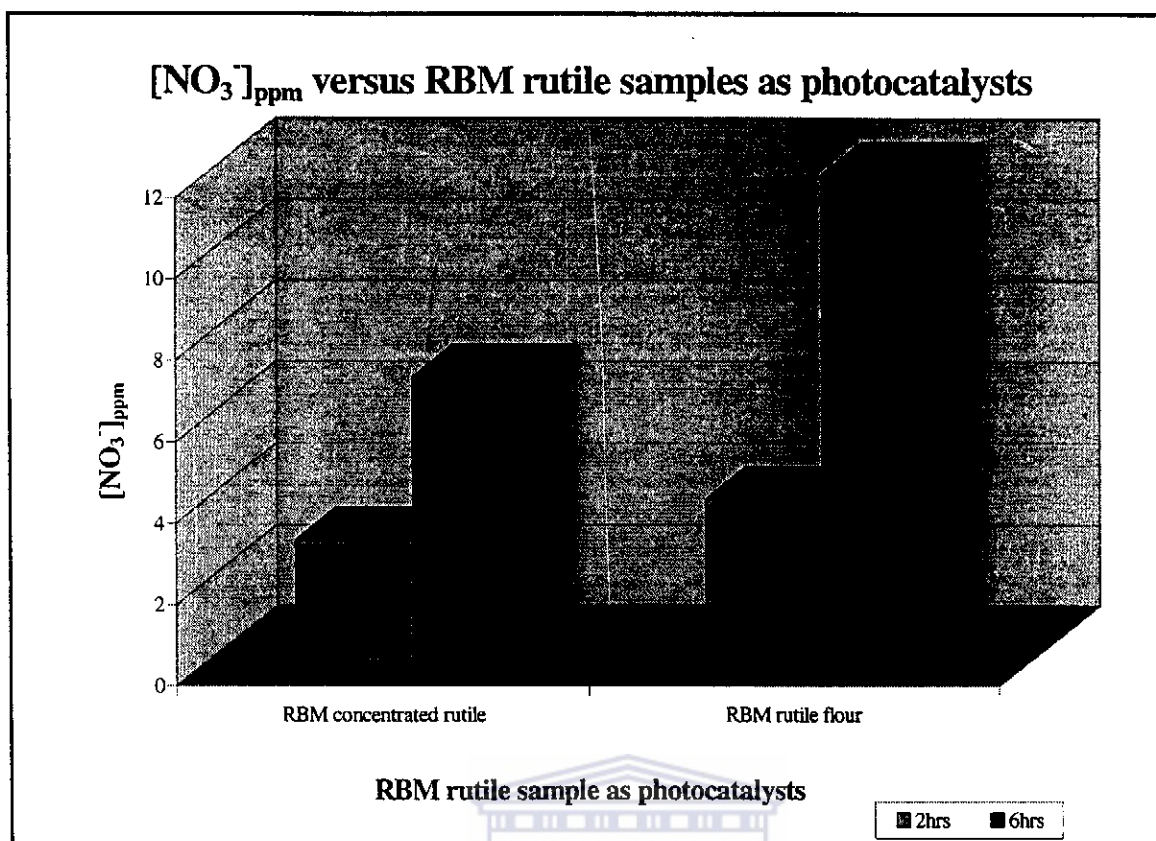


Figure 26: The use of RBM rutile samples as photocatalysts at pH 4. Irradiation was carried out using the Xenon lamp passing air through a 90ml sample at 1500ml/min.

The conditions stipulated above have been applied to the RBM rutile flour and RBM concentrated rutile. The results that were obtained show that the concentration of NO₃⁻ obtained was smaller than that of Degussa P25 photocatalyst. The particle sizes of the RBM samples is greater than that of Degussa P25 and also the purity of the samples in terms of TiO₂ content is much less. However it is interesting that the samples act as photocatalysts for the oxidative fixation of nitrogen. Thus the above industrial products also fix nitrogen under the conditions used.

Chapter 6



Photocatalytic oxidative fixation of dinitrogen has been definitively demonstrated but requires further investigation to establish the mechanism of the reactions involved and to increase the yields of the oxidised products.



Chapter 7

REFERENCES



UNIVERSITY *of the*
WESTERN CAPE

- [1] Wolfe, J.; *Mineral Resources: A world review*; NY; Chapman and Hall; 1984; 169
- [2] Selwood, P. W.; *General Chemistry; Revised Edition*; NY; Henry Holt and company; 1954; 325
- [3] Winchell, A. N.; *Elements of optical mineralogy; an introduction to microscope petrography*; 4th edition; NY; Wiley Ltd.; 1956; 327-331
- [4] McGraw-Hill Encyclopedia of Science and Technology; 6th edition; Mc Graw-hill Book Company; 1987; **18**; 379
- [5] Kotz, J. C.; Purcell, K. F.; *Chemistry and Chemical reactivity*; 2nd edition; NY; Saunders College Publishing; 1991; 113, 977,982-988
- [6] Munoz-Paez, A; *J Chem Educ*; 1994; **71**(5); 38
- [7] Bond, G. C.; *Heterogeneous Catalysis: Principles and Applications*; 2nd edition; Oxford Science Publications; 1987; 40-45
- [8] West, A. R.; *Basic Solid State Chemistry*; Chicester; Wiley Ltd.; 1991; 294-300
- [9] Finklea, H. O.; *J Chem Educ*; 1983; **60**(4); 325
- [10] Linsebigler, A. L.; Lu, G.; Yates, J. T.; *Chem Rev*; 1995; **95**; 735
- [11] Wang, A.; Edwards, J.; Davies, J. A.; *Solar Energy Materials*; 1994; **52**(6); 459
- [12] Vinodgopal, K; Kamat, P. V.; *Chemtech*; 1996; 18
- [13] Mills, A; Davies, R. H.; Worsley, D.; *Chem Soc Rev*; 1993; 417
- [14] Schultz, L.; et al; *Atmospheric Environment*; 1982; **16**; 171
- [15] Kawaguchi, H.; *Environ Tech Lett*; 1984; **5**; 471
- [16] Okamoto, K.; Yamamoto, Y.; Tanaka, H.; Tanaka, M.; Itaya, A.; *Bull Chem Soc Jpn*; 1985; **58**; 2015
- [17] Augugliaro, V.; Palmisano, L.; Sclafani, A.; Minero, C.; Pelizzetti, E.; *Toxicology Environmental Chemistry*; 1988; **16**; 89
- [18] Matthews, R. W.; *Journal of Catalysis*; 1986; **97**; 565

- [19] Matthews, R. W.; *Water Res*; 1986; **20**; 569
- [20] Al Sayyed, G. H.; Pichat, P.; Proc IUPAC Symp Photochem; 12th; 1986; 126
- [21] Sclafani, A.; Palmisano, L.; Davi, E.; *New J Chem*; 1990; **14**; 265
- [22] Sclafani, A.; Palmisano, L.; Schiavello, M.; *J Phys Chem*; 1990; **94**; 829
- [23] Kobayatawa, K.; Nakazawa, Y.; Ikada, M.; Sato, Y.; Fujishima, A.; *Ber Bunsen-Ges Phys Chem*; 1990; **94**; 1439
- [24] Camprostrini, R.; Carturan, G.; Palmisano, L.; Schiavello, M.; Sclafani, A.; *Mater Chem Physics*; 1994; **38**; 277
- [25] Bickley, R. I.; Javanty, R. K.; *J Chem Soc: Faraday Discuss*; 1974; **58**; 194
- [26] Morterra, C. J.; *J Chem Soc: Faraday Trans*; 1; 1988; **84**; 1617
- [27] Primet, M.; Pichat, P.; Mathieu, M. V.; *J Phys Chem*; 1971; **75**; 1216
- [28] Bickley, R. I.; Stone, F. S.; *Journal of Catalysis*; 1973; **31**; 389
- [29] Boonstra, A. H.; Mutsaers, C. A.; *J Phys Chem*; 1975; **79**; 1694
- [30] Courbon, H.; Pichat, P.; Sclafani, A.; Proceedings of "EUROPCAT-F", Montpellier, France, September 12-17; 1993; 727
- [31] Sclafani, A.; Hermann, J. M.; *J Phys Chem*; 1996; **100**; 13655
- [32] Schrauzer, G.N.; Guth, T.; Salehi, J.; Strampach, N.; Liu Nan Hui; Palmer, M.; in *Homogeneous and Heterogeneous Photocatalysis*; E. Pelizzetti and N. Serpone, Eds. NATO ASI Ser., Ser. C.; No. 174; D.Reidel, Hingham, MA; 1986; 509
- [33] Davies, J. A.; Boucher, D. L.; Edwards, J. G.; *Advances in Photochemistry*; John Wiley & Sons, Inc.; 1995; **19**; 235
- [34] Fujishima, A.; Honda, K.; *Nature*, 1972; **238**; 37
- [35] Fujishima, A.; Honda, K.; *Bull Chem Soc Jpn*; 1971; **44**; 1148
- [36] Curtis, H.; *Biology*; 4th Edition; Worth Publishers Inc., NY; 1985; 627-629; 988

- [37] Green, N. P. O.; Stout, G.W.; Taylor, D. J.; Biological Science; 2nd edition; Cambridge University Press; 1990; 281-3
- [38] Starr, C.; Taggart, R.; Biology: Unity and Diversity of Life; 4th edition; Wadsworth Publishing Company, California; 1985; 706-708
- [39] Postgate, J.; *New Scientist*; 1990; **3**; 57
- [40] Taylor, J.; Price, G.; Biology; 1st edition; Harper Collins Publishers; 1997; 218
- [41] Inoue, I.; Fujishima, A.; Konishi, S.; Honda, K.; *Nature*; 1979; **277**, 637
- [42] Hirano, K.; Inoue, K.; Yatsu, T.; *J Photochem Photobiol A: Chem*; 1992; **64**, 255
- [43] Ishintani, O.; Inoue, C.; Suzuki, Y.; Ibusuki, T.; *J Photochem Photobiol A: Chem.*; 1993; **72**, 269
- [44] Schrauzer, G. N.; Guth, T. D.; *J Am Chem Soc*; 1977; **99**; 7189
- [45] Miyama, H.; Fujii, N.; Nagae, Y.; *Chem Phys Lett*; 1980; **74**; 523
- [46] Li, Q.; Domen, K.; Naito, S.; Onishi, T.; Tamaru, K.; *Chem Lett*; 1983; **1983**; 321
- [47] Bickley, R. I.; Vishwanathan, V.; *Nature*; 1979; **280**; 306
- [48] Navio, J. A.; Real, C.; Bickley, R.; *Surface and interface analysis*; 1994; **22**; 417
- [49] Ranjit, K. T.; Vishwanathan, B.; *Indian Journal of Chem*; 1996; **35A**; 443-453
- [50] Endoh, E.; Lehend, J. K.; Bard, A. *J Phys Chem*; 1986; **90**; 6223
- [51] Ileperuma, O. A.; Weerasinghe, F. N. S.; Lewke Bandara, T. S.; *Solar Energy Materials*; 1989; **19**; 409
- [52] Hori, Y.; Nakatsu, A.; Suzuki, S.; *Chem Lett*; 1985; 1429
- [53] Bickley, R. I.; Jayanty, R. K. M.; Vishwanathan, V.; Navio, J. A.; Homogeneous and Heterogeneous Photocatalysis; E. Pelizzetti and N. Serpone (Reidel, Dordrecht); 1986; 555
- [54] Bickley, R. I.; Day, R.; Vishwanathan, V.; Proc 9th Intl Cong Catal; edited by M J Phillips and Terman; **4**; 1988; 1505

- [55] Mac Lean, W. Ritchie, M.; *J Appl Chem*; 1965; **15**; 452
- [56] Connor, J. A.; Ebsworth, E. A. V.; *Adv Inorg & Radio Chem*; 1964; **6**; 286-290
- [57] Jere, G.; Patel, C.; *Zeitschrift fur anorganische und allgemeine chemie*; 1962; 175
- [58] Schwarz, R.; Giese, H.; *Z Anorg Allg Chem*; 1928; **176**; 209
- [59] Skoog, D. A.; West, D. M.; Holler, F. J.; *Fundamentals of Analytical Chemistry*; 6th Edition; Saunders College Publishing; 1992; 593
- [60] Theophanides, T.; *Fourier Transform Infrared Spectroscopy*; D. Reidel Publishing Company; 1984; 55-60
- [61] Skoog, D. A.; Leary, J. J.; *Principles of instrumental analysis*; 4th Edition; Saunders College Publishing; 1992; 137-138
- [62] Goodhew, P. J.; Humphreys, F. J.; *Electron Microscopy and Analysis*; 2nd edition; Wykeham Publications Ltd.; 1988; 106, 154, 160-163
- [63] Boltz, D. F.; *Ultraviolet spectrometry*; 23-24
- [64] Svehla, G.; *Vogel's qualitative inorganic analysis*; John Wiley & Sons Inc.; 1987; 163; 182-185
- [65] Bischoff, M.; Hiar, A.; Turco, R.; *Commun Soil Sci Plant Ana*; 1996; **27**; 2765
- [66] Piccini, A.; *J Chem Soc*; 1882; **A42**; 809
- [67] Weller, A.; *J Chem Soc*; 1883; **A44**; 295
- [68] Levy, L.; *C R hebd Séances, Acad Sci*; 1889; **108**; 294
- [69] Mc Kinney, R.; Madson, W.; *J Chem Educat*; 1936; **13**; 155
- [70] Kharkar, D. P.; Patel, C. C.; *Current Sci*; 1955; **21**; 413
- [71] Partington, J. R.; Fatallah, A. H.; *J Chem Soc*; 1950; 1931



UNIVERSITY *of the*
WESTERN CAPE